KTH ROYAL INSTITUTE
OF TECHNOLOGY

Doctoral Thesis in Fiber and Polymer Science

Textile and Paper Microfluidic Platforms for Electroanalytical Nucleic Acid Testing

SHIRIN KHALILIAZAR

Stockholm, Sweden 2021

Textile and Paper Microfluidic Platforms for Electroanalytical Nucleic Acid Testing

SHIRIN KHALILIAZAR

Academic Dissertation which, with due permission of the KTH Royal Institute of Technology, is submitted for public defence for the Degree of Doctor of Philosophy on Monday 18th October, at 14:00. in Kollegiesalen, KTH, Brinellvägen 8, Stockholm. The defence will be in English. Opponent: Doctor Firat Güder, from Imperial College London, England.

Doctoral Thesis in Fiber and Polymer Science
KTH Royal Institute of Technology
Stockholm, Sweden 2021

ISBN 978-91-7873-966-0
TRITA-CBH-FOU-2021:33

Printed by: Universitetsservice US-AB, Sweden 2021

Dedicated to my Family

Human beings are members of a whole

In creation of one essence and soul

If one member is afflicted with pain

Other members uneasy will remain

If you have no sympathy for human pain

The name of human you cannot retain

Saadi Shirazi

Abstract

Rapid and accurate near-patient diagnostic tests outside well-equipped laboratories are essential in the fight against outbreaks of infectious diseases, especially when these can turn into pandemics. As severe acute respiratory syndrome CoV 2 (SARS-CoV-2) is the latest but probably not the last pandemic of the 21st century.

Nucleic acid amplification tests (NAATs) identify pathogens at the molecular level by targeting specific gene sequences. NAATs are currently the gold standard of molecular diagnostics, given their reliability, sensitivity, and specificity. In addition, NAATs can provide quantitative results with a short turnaround time compared to conventional immunoassays or culturing methods. However, most NAATs necessitate centralized laboratories and trained health professionals and, to a large extend, fail to be point-of-care (POC).

The biosensing field was inspired by the microelectronics revolution in the 1980s, which led to the emergence of the micro-total analysis systems (μTAS) concept. μTAS was envisioned to miniaturized laboratory-based tests in single microfluidic devices. The combination of POC NAATs with μTAS can offer rapid, sensitive, and specific diagnostic tools of great importance in tackling diseases.

In this thesis, we have utilized paper and textile materials as a platform for developing μTAS. These materials possess many features necessary for advanced μTAS, such as the ability to transport liquids, store reagents and embed electronic functions, making them ideal for integrating affordable, portable, and easy to manufacture μTAS for NAATs.

We have specially developed NAATs with paper-based and thread-based electrochemical readout to provide quantitative responses with high sensitivity, specificity, and the possibility to connect to portable digital electronics. This work paves the way for robust sample-to-answer digital POC NAATs.

Sammanfattning

Snabba och noggranna diagnostiska tester som utförs nära patienten utanför välutrustade laboratorier är det mest avgörande sättet att ta itu med smittsamma sjukdomar, som i värsta fall kan förvandlas till en pandemi. Severe acute respiratory syndrome coronavirus 2 (SARS-CoV2) är den senaste men förmodligen inte den sista pandemin under 2000-talet.

Nukleinsyraamplifieringstest (NAAT) identifierar patogener på en molekylär nivå genom att rikta in på specifika gensekvenser. NAAT är för tillfället den gyllene standarden för molekylär diagnostisk teknik med tanke på dess tillförlitlighet, känslighet, och specificitet Utöver detta ger NAAT kvantitativa resultat med en kort behandlingstid i motsats till konventionella immunanalyser eller odlingsmetoder. De flesta NAAT-metoder kräver dock centraliserade laboratorier och utbildad personal och är därmed inte anpassade för självtest nära patienten.

Biosensorsfältet var inspirerat av mikroelektronikrevolutionen på 1980-talet, vilket ledde till uppkomsten av konceptet mikrototalanalyssystem (μTAS). Dessa system har som syfte att miniatyrisera laboratoriebaserade tester genom att utföra alla steg i enstaka mikrofluidanordningar. Kombineringen av patientnära NAAT-tester med μTAS kan därför erbjuda snabba, känsliga och specifika diagnostikverktyg och därmed ha stor påverkan för att förhindra överföring av infektionssjukdomar.

I den här avhandlingen har vi använt papper och textila material som en platform utveckling av μTAS.Dessa material har många egenskaper som är nödvändiga för μTAS såsom förmågan att transportera vätskor, lagra reagenser och att integrera elektroniska funktioner, vilket gör dem ideala för att integrera prisvärda, bärbara och lättillverkade μTAS för NAAT-tester.

Vi har speciellt utvecklat NAAT-tekniker med papper- och trådbaserad elektrokemisk avläsning som ger kvantitativa svar med hög känslighet, specificitet och möjlighet att ansluta till bärbara elektroniska enheter. Detta arbete banar vägen för robusta, digitala och patientnära prov-till-svar-tester som baseras på NAAT-teknik.

List of Publications

This thesis is a summary of the following papers:

I. Chondrogiannis, G., **Khaliliazar, S.,** Toldrà, A., Réu, P., & Hamedi, M. M. (2021). Nitrocellulose-bound achromopeptidase for point-of-care nucleic acid tests. *Scientific reports*, *11*(1), 1-7.

II. **Khaliliazar, S.,** Ouyang, L., Piper, A., Chondrogiannis, G., Hanze, M., Herland, A., & Hamedi, M. M. (2020). Electrochemical detection of genomic DNA utilizing recombinase polymerase amplification and stem-loop probe. *ACS omega*, *5*(21), 12103-12109.

III. **Khaliliazar, S.,** Öberg Månsson, I., Piper, A., Ouyang, L., Réu, P., & Hamedi, M. M. (2021). Woven Electroanalytical Biosensor for Nucleic Acid Amplification Tests. *Advanced Healthcare Materials*, *10*(11), 2100034.

IV. *** Khaliliazar, S.,** * Toldrà, A., Chondrogiannis, G., & Hamedi, M. M. (2021). Electroanalytical Paper-based Nucleic Acid Amplification Tests with Integrated Thread Electrodes. Submitted.

*Shared first authorship

Author contributions

The appended papers are collaborations with my co-authors, and my contributions are described below:

I. Second Author: Designing and screening RPA primers, providing support in experimental work, data analysis and revising the manuscript.

II. First Author: Planning and performing all experiments, analyzing the results, and writing the manuscript.

III. First Author: Planning and performing all experiments, analyzing the results, and writing the manuscript.

IV. Co-First Author: Contributing equally in planning, performing all experiments, analyzing the results, and writing the manuscript.

Scientific contributions not included in this thesis

I. Xia, J., **Khaliliazar, S.,** Hamedi, M. M., & Sonkusale, S. (2021). Thread-based wearable devices. *MRS Bulletin*, 1-10.

II. Piper, A., Månsson, I. Ö., **Khaliliazar, S.,** Landin, R., & Hamedi, M. M. (2021). A disposable, wearable, flexible, stitched textile electrochemical biosensing platform. *Biosensors and Bioelectronics*, 113604.

III. Ouyang, L., Buchmann, S., Benselfelt, T., Musumeci, C., Wang, Z., **Khaliliazar, S.,** Tian, W., Li, H., Herland, A., & Hamedi, M. M. (2021). Rapid Prototyping Heterostructured Organic Microelectronics using Wax Printing, Filtration, and Transfer. Submitted manuscript. *Journal of Materials Chemistry C.* In Press

IV. Toldrà, A., Ainla, A., **Khaliliazar, S.,** Chondrogiannis, G., Réu, P., & Hamedi, M. M. (2021). Detection of isothermally amplified DNA on printed circuit boards with a homemade portable potentiostat. Manuscript.

Abbreviations

µPAD	Microfluidic paper-based analytical device
µTADs	Microfluidic thread/textile-based analytical devices
µTAS	Micro total analysis systems
6-MCH	6-Mercapto-1-hexanol
ACP	Achromopeptidase
bp	Base pair
CA	Chronoamperometry
CL	Chemiluminescence
CV	Cyclic voltammetry
DNA	Deoxyribonucleic acid
DPV	Differential pulse voltammetry
dsDNA	Double-stranded DNA
ECL	Electrochemiluminescence
E-DNA sensor	Electrochemical DNA sensor
FL	Fluorescence
HDA	Helicase-dependent amplification
HIV	Human immunodeficiency viruses
HRP	Horseradish peroxidase
$K_3 Fe(CN)_6$	Potassium ferricyanide
LAMP	Loop-mediated isothermal amplification
MB	Methylene blue
MDA	Multiple displacement amplification
MRSA	Methicillin-resistant *Staphylococcus aureus*
NAATs	Nucleic acid amplification tests
NASBA	Nucleic acid sequence-based amplification
PCR	Polymerase chain reaction
PDMS	Polydimethylsiloxane
PET	Polyethylene terephthalate
RCA	Rolling circle amplification
RPA	Recombinase polymerase amplification
SEM	Scanning electron microscope
S-L probe	Stem-loop probe
ssDNA	Single-stranded DNA
SWV	Square wave voltammetry
POC	Point-of-care
TCEP	Tris(2-carboxyethyl) phosphine
TMB	3,3′,5,5′-Tetramethylbenzidine

Table of Contents

1 Purpose of the study

*"Without a diagnosis, medicine is blind"**

Infectious diseases and antibiotic-resistant infections are among the main causes of death worldwide and can severely burden societies' economies and psychological health. These life-threatening pathogens such as methicillin-resistant *Staphylococcus aureus* (MRSA), Ebola, Zika, MERS-CoV, and most recently, SARS-CoV-2, evidently and realistically indicated the significance of rapid and early diagnosis to prevent transmission of infectious pathogens and enable early patient isolations.

Molecular diagnostic techniques, namely nucleic acid tests (NAATs), are the gold standard for detecting outbreaks that detect pathogen-specific nucleic acid sequences with high sensitivity and specificity and a short time for identifying new mutations. The current NAATs, however, rely on centralized laboratories with trained personnel that make them inapplicable to POC diagnosis, in which the diagnostic tests are carried out outside clinical laboratories, at home individually, or by minimally trained healthcare personnel.

Micro total analysis systems (μTAS) have paved the way for POC diagnosis by miniaturizing the diagnostic tests in microfluidic devices. According to the established ASSURED criteria by World Health Organization, μTAS for POC tests need to be Affordable, Sensitive, Specific, User-friendly, Rapid and robust, Equipment-free, and Deliverable to end-users.

Paper and textile materials are interesting and high-potential candidates for developing POC NAATs. These inexpensive porous materials benefit from inherent characteristics such as wicking, which eliminates the need for external pumps for fluid control, printability, weaving, knitting, and sewing. The latter is specific for textiles that offer at scale, easy manufacturing of the microfluidic devices without the need for microfabrication processing. Additionally, paper and textiles provide extensive opportunities for integrating electrochemical DNA sensors for sensitive and specific detection.

*Dr. Lee Schroeder (*University of Michigan*), Dr.Timothy Amukele (J*ohns Hopkins School of Medicine*) and Dr. Madhukar Pai (*McGill Global Health Programs*)

The main goal of this study was to investigate and develop integrated electrochemical DNA biosensors in paper and thread-based microfluidic devices as quantitative, sensitive, and specific POC NAATs.

This aim was in line with the United Nations' sustainable development goals (SDGs)** by 2030, "*Good Health and Well-being*" as goal number 3, which necessitates reducing mortality from communicable and non-communicable diseases by prevention, diagnosis, and treatment to promote mental health and well-being. Furthermore, using paper and textile as sustainable materials for developing affordable and biodegradable microfluid diagnostic devices without the need for non-eco-friendly microfabrication processes leads to economically, environmentally, and socially sustainable products.

** United Nations,. "*Take Action for the Sustainable Development Goals*." from https://www.un.org/sustainabledevelopment/sustainable-development-goals/

2 Introduction

2.1 Micro Total Analysis Systems (μTAS)

Micro total analysis systems, also known as lab-on-a-chip (LOC), are microfluidic, analytical miniaturized devices capable of performing multiple sample analysis steps.[1] This concept was derived from the miniaturization techniques developed for microelectronics in the 1980s. Here the microfluidic devices were envisioned to process small quantities of fluids (10^{-6} to 10^{-18} L), using channels with the dimension of tens to hundreds of micrometers.[2] [3]

Microfluidic devices offer remarkable advantages over conventional bench-top (macro-scale) systems for various applications, including diagnostics, environmental monitoring, drug discovery, and forensic science. The advantages[4] include; (1) small quantities (microliter in volume) of samples and reagent; (2) short time of analyses because of short diffusion distances and high surface to volume ratios; (3) low power demands to operate; (4) compact designs that allow multiplex target analysis in a single device; and (5) portability, which makes the μTAS outstanding candidates for (POC) applications, where proper laboratory access is limited, see Figure 1.[5]

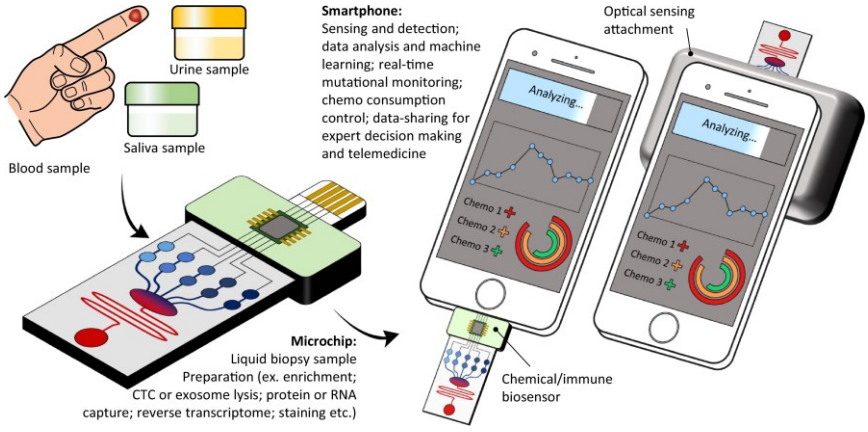

Figure 1. An integrated microfluidic diagnostic device with smartphones for POC applications. Reproduced with permission from Reference [5]. © 2018 Elsevier.

2.2 µTAS for Point-of-Care (POC) Tests

The term point-of-care (or need) test was introduced as near the patient or on-site diagnostics, a paradigm shift from conventional diagnostic tests conducted in centralized clinical laboratory settings to bedside tests. POC diagnostics are of significant importance for the control and monitoring life-threatening pathogens like Zika virus, Ebola virus, or most recently, SARS-CoV-2. POC tests deliver timely diagnostics and monitoring, which enable early and rapid detection of infectious diseases, which may lead to high transmission rates and mortality.[6] The World Health Organization (WHO) issued a guideline named ASSURED in 2015, in which criteria for selecting an efficient POC testing are presented. ASSURED is an acronym for Affordable, Sensitive, Specific, User-friendly, Rapid and Robust, Equipment-free, and Delivered to the greatest need. Microfluidic POC diagnostic devices potentially fulfill the ASSURED criteria by providing portable, low-cost, rapid, and robust testing devices.[7] Microfluidic POC diagnostic tests consist of three steps: (1) a sample collection and pre-analytical step; (2) an analytical step involving detection of target and further transformation into a measurable signal; and (3) a post-analysis step, involving read-out and data analysis followed by data storage and transmission.[8] The latter can be facilitated by merging microfluidic POC devices with smartphone-based technologies for cloud computing system.[9] Contrary to the recent developments and progress in the µTAS POC diagnostics, various challenges must still be addressed in the all three aforementioned steps to develop fully automated, sample-to-answer POC microfluidic diagnostic devices.[10]

2.3 POC Nucleic Acid Amplification Tests (NAATs)

Molecular diagnostics and immunoassays are common diagnostic techniques in the fast-paced medical world that have a much quicker turnaround time compared to traditional plating methods, which require several days of cell culturing.[11]

Immunoassays generally rely on specific antibodies binding to unique antigens on the surface of pathogens, while molecular diagnostic methods target genetic materials (DNA or RNA) inside pathogens´ cells at the molecular level.[12] NAATs are molecular diagnostic methods that in principle consist of the following particular steps: (1) lysis of pathogens cells to extract nucleic acids; (2) purification and isolation of the extracted nucleic acids from

the lysates that may inhibit the downstream reactions; (3) amplification of the purified and isolated nucleic acids, in which target genes are replicated up to billions of copies; and (4) detection of the amplified target gene using optical, colorimetric, chemiluminescence or electrochemical methods. Conventional NAATs such as PCR and qPCR heavily rely on bulky laboratory equipment like thermocyclers, gel electrophoresis, or optical systems, which are unsuitable for POC tests.[13]

Microfluidic POC NAATs have paved the way to adapt the conventional molecular diagnostic methods for rapid, low-cost, and portable tests.[14] Microfluidic POC NAATs provide higher levels of specificity, using well-designed primers, as they target a unique gene sequence in pathogens nucleic acids, compared to POC immunoassay tests (including lateral flow COVID-19, or HIV salvia antibody test), which may result in false-positive test results due to possible cross-interaction between similar protein complexes to target antigens and specific antibodies. Additionally, NAATs offer higher sensitivity than immunoassay tests, as they enable the detection of a few single copies of the target sequence in a sample at the very early stage of infection,[15] thanks to the DNA amplification step, see Figure 2.[16]

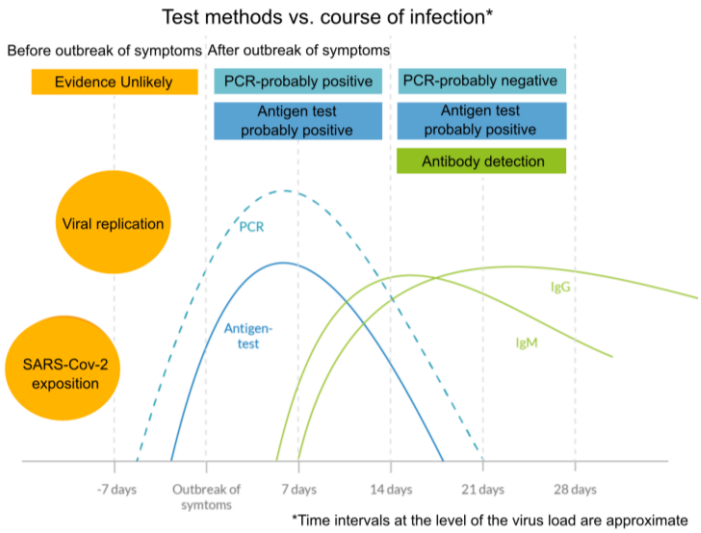

Figure 2. Overview of clinical laboratory techniques including nucleic acid amplification tests (PCR), immunoassays (antigen tests), and serology tests (antibody tests) for COVID-19 pandemic. Adapted from Reference [16].

2.4 Paper and Textile "Fiber-based" platforms for NAATs

Papers, threads, and textiles are fiber-based materials that offer remarkable advantages over silicon, glass, and polymers (e.g., PDMS) for fabricating low-cost, portable, user-friendly, and scalable microfluidic POC devices, see Figure 3.[17,18] More importantly, fiber-based materials wick liquids through capillary action, eliminating the need for external equipment such as pumps to flow fluids in microfluidic devices.[19,20]

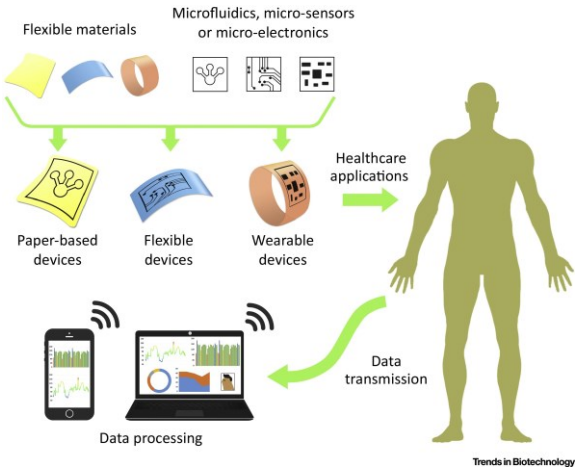

Figure 3. Overview of paper-based and textile-based analytical microfluidic devices. Reproduced with permission from Reference [18]. ©2016 Elsevier.

2.4.1 Paper and textile features in POC NAATs

Microfluidic paper-based analytical devices (μPADs) were popularized by the Whiteside group and have gained interest in the biosensing field.[21] Paper is considered as a desirable substrate for developing NAATs due to its six key attributes:[22]

(1) **Storing reagents**: the porous network of paper enables storage of reagents like DNA and proteins in dried/freeze-dried form for further reactions or easy transportation of reagents at room temperature without the need for cold chain logistics.

(2) **Transporting fluids**: capillary forces in the paper make the flow of fluids in the substrate independent of external forces. Capillary forces result from two opposing forces: cohesion forces and adhesion forces. The adhesion forces govern the interactions

between paper substrate and contacting surface of the fluid. The cohesion forces are defined as intermolecular interactions between liquid molecules at the liquid-air interface when fluid is introduced to the paper substrate, and adhesion forces are between the solid-liquid at the interface. The adhesion forces are in charge of spreading the liquid into the paper substrate, while the cohesion forces such as surface tension minimize the area between liquid and air at the interface. Once the adhesion force dominates the cohesion force, the fluid starts wicking in the porous substrates. The wicking property of porous substrates can be affected or tuned by several factors, including paper materials, structures, pore sizes, shapes and the physicochemical properties of the liquid.

(3) **Printing**: paper substrates can be readily printed by conductive inks, pastes, or wax to create paper-based electorates and microfluidic channels. [23]

(4) **Filtering**: paper can have pore sizes ranging between 2-100 μm,[24] depending on their types and applications. This intrinsic characteristic has made the paper a prominent candidate for chromatography and extraction processes, in which paper absorbs different species and allows molecules smaller than its pore size to flow downstream. Thus, the filtering feature of paper can make it a potential substrate for sample preparation for analytical purposes.

(5) **Concentrating:** due to the high surface to bulk ratio, liquids can easily evaporate from the paper substrates. This can have a beneficial effect to concentrate analytes and also a detrimental effect on the evaporation of reaction media if there is no good sealing of the paper-based device.

(6) **Valving**: this is the function that enables the control of liquid in paper substrates during multi-step reactions. Valves can be realized in μPADs using simple folding, cutting, mechanical displacement, or locally chemical/physical modifications in its designed structure.[25]

Microfluidic thread/textile-based analytical devices (μTADs) are relatively new, smart, and simple technologies for at scale production of ASSURED POC analytical devices.[26] Similar to μPADs, μTADs benefit from the wicking properties of textiles and threads due to capillary forces caused by the gaps between fibers. Contrary to μPADs, threads and textiles can be readily transformed into 3D-microfluidic devices using textile architectures with fabrication methods including sewing, weaving, and knitting. Threads as

flexible materials can also be easily integrated into wearable microfluidic analytical devices. [27]

Fibers are the building blocks of μTADs and can be divided into two categories: natural and synthetic. Natural fibers, including cotton, silk, and wool, are typically covered with a wax layer (long fatty acid chains) that impede the flow of fluid along with the threads/yarns by reducing the wettability of the fibers. To address this, different surface treatments, including plasma modification and scouring in NaOH or Na_2CO_3, are employed to remove wax layers from the natural fibers. [20]

Alternatively, synthetic fibers can be engineered to provide significant wicking properties. Coolmax® yarns are commercial polyester (polyethylene terephthalate, PET) fibers specifically engineered to quickly wick and dry 5-200 times faster than cotton fibers. [28]

2.4.2 Sample preparation in fiber-based POC NAATs

Preparation and pretreatment of biological samples, including blood, urine, and salvia, is a key step in NAATs, which involves removing components that can inhibit downstream processing.[29] Sample preparation in NAATs includes collection, storage, extraction, and purification of nucleic acids. Traditionally, sample preparations in clinical laboratories are performed using solid-phase extraction, electrostatic interactions, or sequence-specific capturing methods. The solid-phase extraction with silica particles is the most common method used to date. The conventional sample preparation methods require laboratories with trained personnel, and the processes are generally tedious and time-consuming. [30]

There has been a lot of progress in translating these laboratory-based procedures into POC diagnostic platforms.[30] FTA® cards (Flinders Technology Association) are a well-known commercialized sample preparation technology for POC NAATs.

FTA® cards are the most prevalent paper-based products for sample preparation in molecular diagnostic techniques. These are chemically modified cellulose papers that enable safe sample collection, storage at room temperature for a long period (over five years for collected DNA), protection

of nucleic acids from degradation by proteins present in the sample, UV radiations, and oxidation. The stored nucleic acids can be isolated, purified, and prepared for downstream NAATS phases, using the steps shown in Figure 4.[31,32]

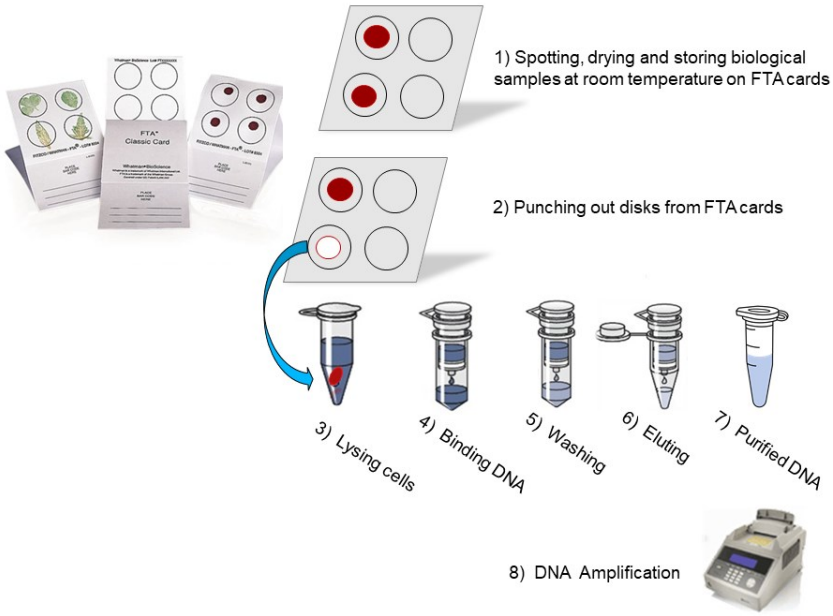

Figure 4. Overview of sample preparation steps using FTA cards in NAATs. Adapted with permission from Reference [31]. © 2015 John Wiley and Sons.

Several groups have presented paper-based sample preparation methods. Byrnes et al. developed a paper-based device using chitosan-coated nitrocellulose and glass fiber substrates for simultaneous purification and concentration of DNA from blood.[33] Govindarajan et al. presented a paper-based origami that lyses bacterial cells and extracts DNA from pig mucins (spiked with *Escherichia coli*) at room temperature by folding different reaction zones in the device using a home-made buffer. [34]

Some of the reported paper-based sample preparation systems rely on the filtration capacity of paper. Kolluri et al. fabricated a paper-and-plastic device named SNPflax to extract and purify nucleic acid from a whole blood sample.

This device consists of a glass fiber-capture membrane to collect purified nucleic acids and a chromatography paper, guiding the sample towards glass fibers through capillary forces.[35] Mcfall et al. used isolation techniques in the paper substrate to capture and concentrate DNA from blood samples by adding NaOH solution to a glass fiber disk. The samples were chemically lysed using a Triton-X solution and added to the glass substrate. The glass fiber disk, which contained the sample, was directly used in tube-based PCR reactions or as templates in the qPCR method.[36] Sullivan et al. reported a paper-based device based on isotachophoresis (ITP) for nucleic acid separation and purification from blood cells for NAATs. The device operated under a discontinuous electrical field provided by high electrophoretic mobility- leading electrolyte (LE) and low mobility, trailing electrolyte (TE). By applying an electric field to the device, molecules such as nucleic acids with intermediate mobility concentrate at the interface of the two electrolytes, and species like proteins with higher/lower mobility than the buffers, were excluded from the interface. This process resulted in concentrating purified DNA in the paper-based substrate at the interface of the two buffers. [37]

These reported devices and the commercial FTA cards, however, require multiple steps of processing and manual intervention, which are still existing challenges for integrating sample pretreatment steps in microfluidic fiber-based POC NAATs.[38]

2.4.3 Isothermal amplification in fiber-based POC NAATs

Nucleic acid amplification is a vital and central step in NAATs. This step contributes significantly to the sensitivity of NAAT tests, as nucleic acid amplification methods generate abundant copies of target sequences from biological samples that typically contain a few copies of target cells not sufficient for direct detection.[39]

Polymerase chain reaction (PCR) is the most common and widely used nucleic acid amplification method in clinical laboratories. It is known as the gold standard technique due to its high sensitivity, specificity, and available online tools for designing its primers. PCR is a temperature-dependent reaction (see Figure 5) that requires thermocyclers for accurate temperature cycling (rapid heating and cooling between 50-95°C). This feature currently limits PCR in paper-based POC NAATs.[40,41] Because of this shortcoming,

isothermal amplification methods have been introduced as potential alternatives to PCR in POC NAATs.[42]

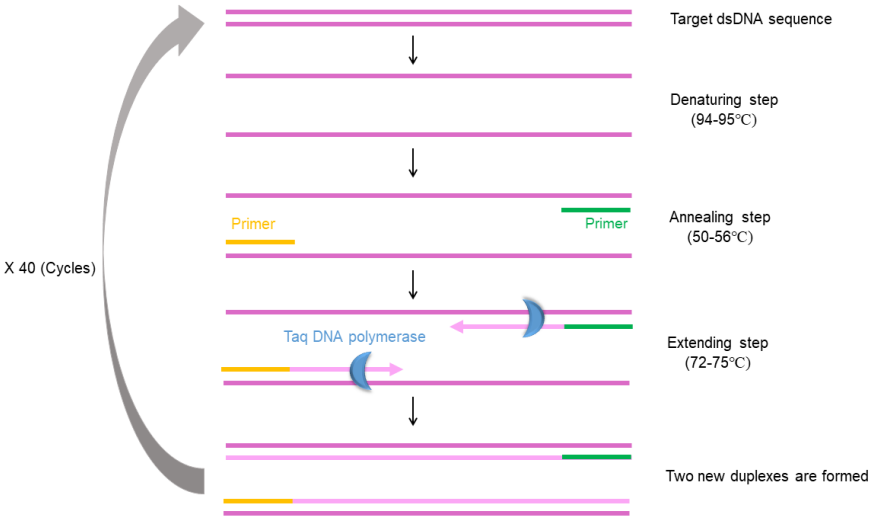

Figure 5. Illustration of steps of polymerase chain reaction (PCR).

Several isothermal amplification methods have been reported, including loop-mediated isothermal amplification (LAMP), recombinase polymerase amplification (RPA), rolling circle amplification (RCA), nucleic acid sequence-based amplification (NASBA), helicase-dependent amplification (HDA), and multiple displacement amplification (MDA), which all work at a constant temperature making them more adaptable in microfluidic fiber-based POC NAATs. [43] [44]

Among these methods, LAMP and RPA are the two most reported methods in paper-based POC NAATs. They both exploit strand-displacement activity of a DNA polymerase enabling cyclic amplification without the need for a denaturation step at 95°C, a must in PCR.[45] [46]

LAMP is a rapid (15-60 minutes) isothermal amplification technique that functions using six primers at 65°C.[47] Linnes and coworkers systematically characterized different porous substrates, including cellulose, glass fiber, nitrocellulose, polyethersulfone (PES), and polycarbonate (PC), for

conducting LAMP, using four separate DNA and RNA targets. The results showed efficient LAMP reactions in the PES while the other substrates inhibited the reactions.[48] In another study, Rodriguez et al. reported paper-based POC NAATs, which featured *in-situ* LAMP amplification in a PES membrane. The device could amplify extracted RNA from patient samples in 45 minutes with a limit of detection of 10^6 copies/mL.[49]

Unlike LAMP, RPA requires only two primers, operates at relatively low constant temperatures (37-42°C), and can yield products in less than 30 minutes. Figure 6 illustrates the step-wise mechanism of the RPA reaction. Also, some studies show that RPA even works with PCR primers, which are usually shorter (18–30 bases) than RPA primer length (30–38 bases). These properties make RPA a desirable candidate for paper-based POC NAATs.[50] Rohrman and Richards-Kortum developed a paper-based device using different layers of glass fibers, cellulose papers, and plastics to conduct RPA reactions for HIV samples. The device amplified 10 copies of target DNA in 15 minutes using freeze-dried RPA pellets in the porous reaction zone. The RPA products were later detected by colorimetric lateral flow strips. They also reported that the glass fiber is the most compatible substrate over GF/DVA, MF1, VF2, and Fusion 5 Whatman membranes[51] for RPA reaction, as it provided amplicons with a minimum primer-dimer formation (primer-dimers are nonspecific amplicons seen as noise in gel electrophoresis images). Rohrman and Richards-Kortum hypothesized that the pore size of the glass substrates could allow better diffusion and interaction between the RPA reagents. GF/DVA membrane, which contains some percentage of glass fibers, indicated slightly fewer target products than glass substrates. Cellulose papers, however, showed the lowest RPA efficiency along with the highest noise in the gel electrophoresis image.[52]

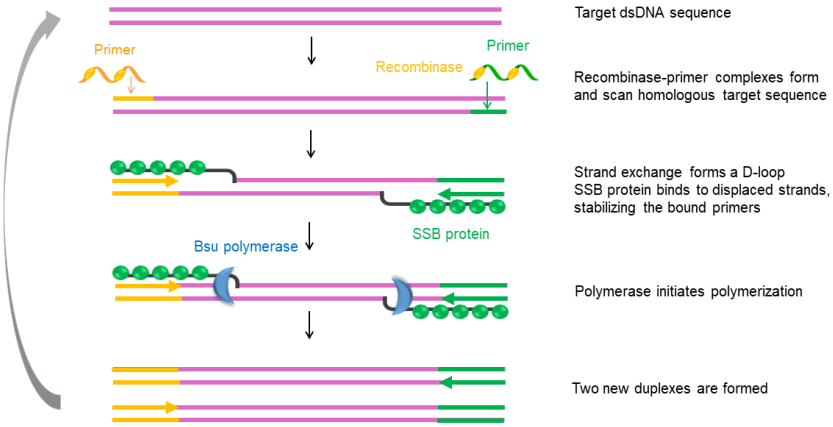

Figure 6. Illustration of the mechanism of recombinase polymerase amplification (RPA).

In another study, Cordy and Richards-Kortum presented a paper-plastic-based device that performed RPA amplification, dilution, and visual detection of the amplified target. The device successfully amplified synthetic plasmodium DNA, which causes Malaria, inside a Whatman Grade 1 paper for as few as 5 copies/µL of the target in less than 30 minutes. [53]

2.4.4 Detection in fiber-based POC NAATs

Paper substrates can be modified or manipulated with various elements for detecting DNAs from nucleic acid amplification in POC NAATs.[54] Colorimetric methods are the most common detection techniques in POC paper and textile-based NAATs due to their simplicity and ease of integration. They provide qualitative/semi qualitative answers that naked eyes can simply read based on the change of colors in reaction zones, see Figure 7.[55] This method, however, suffers from low sensitivity, and its read-out results may vary from person to person because of external lighting conditions. Therefore, external imaging equipment such as digital cameras, phone cameras, or bench-top scanners is employed to capture images of reaction zones for further quantitative analysis using image analysis software ImageJ, for instance.[56-59]

Luminescence techniques, including chemiluminescence (CL), fluorescence (FL), and electrochemiluminescence (ECL), have also been used in µPAD

NAATs. In CL and ECL methods, light emitted from chemical and electrochemical reactions, respectively, are measured. While fluorescence methods necessitate an external excitation source to acquire luminescence.[56,60]

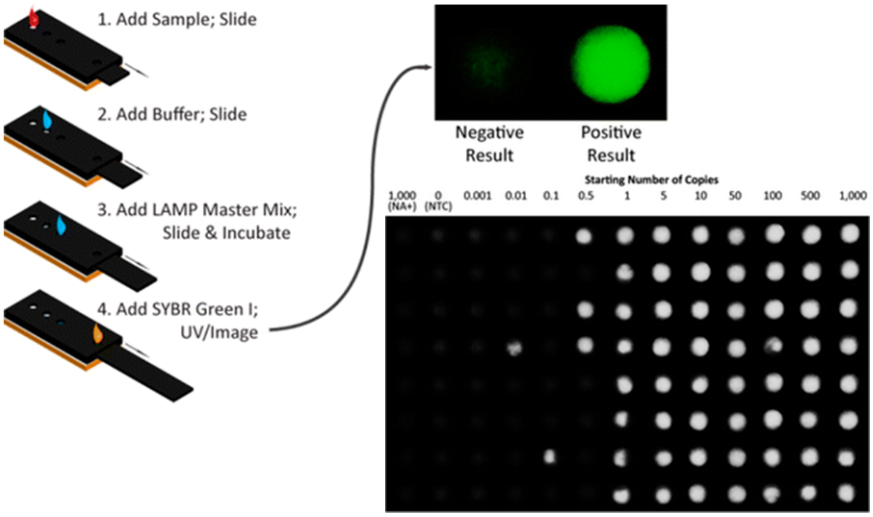

Figure 7. A sample-to-answer integrated paper machine for colorimetric-based detection of *E. coli* from spiked human plasma. Adapted with permission from Reference [55]. © 2015 American Chemical Society.

Electrochemical methods have great advantages over colorimetric and most other detection technologies in µPADs and µTADs. Because they provide quantitative results with high sensitivity and specificity, and they can be easily connected to readily available and portable potentiostats for reliable readout. Furthermore, their results can also be coupled seamlessly to digital systems for data storage, analysis, and transfer.[61,62]

2.5 Electroanalytical DNA biosensors

Electrochemical biosensors translate chemical signals into electrical signals using three main elements, including (1) biorecognition elements, (2) electrodes or transducers, and (3) signal outputs.[63] Contrary to colorimetric detection, electrochemical techniques are not sensitive to environmental illumination conditions and require no manual readout or cameras, leading

to lower sensitivity, lower reproducibility, and higher cost.[64] Different electrochemical techniques measure quantitative electrochemical signals, including chronoamperometry, voltammetry, and electrochemical impedance methods. The chronoamperometric (CA) method measures current changes *vs.* time due to applied potentials (step/pulse form). Voltammetry techniques such as cyclic voltammetry (CV), differential pulse voltammetry (DPV), and square wave voltammetry (SWV) monitor the changes in current as a result of applied potential profile over time. The SWV and DPV provide faradic currents by eliminating the contribution of non-faradic currents caused by double-layer charging, making them highly sensitive. Unlike chronoamperometry and voltammetry methods, impedance techniques quantify changes in dielectric properties of the electrochemical system. [62,65]

Electrochemical hybridization (sequence-specific)- based DNA sensors measure electrochemical changes that occur due to sequence-specific hybridizations between DNA probes (generally between 15-40 base pairs) immobilized on electrodes and target sequences through base-pairing.[61] Figure 8 illustrates three examples of redox-active indicator-based electrochemical DNA probes that yield electrochemical signals due to hybridization-induced changes, based on three mechanisms.[66] [67] Figures 8A and 8B show redox-labeled and enzyme label-based electrochemical DNA biosensors, respectively. The redox-labeled immobilized DNA probes in the presence of target single-stranded DNA (ssDNA) sequence undergo conformation changes altering electron transfer efficiency at the electrode interface due to the DNA probe and complementary target hybridization events. Unlike conformation change-based DNA probes, which mainly requires target single-stranded DNA, sandwich hybridization assay (SHA) shown in Figure 8B enables detection of target double-stranded DNA (dsDNA) that consists of tails at 5´ and 3´ ends, through capture (immobilized on electrode surface) and HRP enzyme-modified reporter probes. These capture and reporter probes are complementary to the tails of target dsDNA. Figure 8C indicates a type of hybridization-based DNA sensor, in which the free redox molecules interact with dsDNA formed by hybridization of target ssDNA with the immobilized DNA probe on the electrode. Redox molecules interact with dsDNA/ssDNA through electrostatic, intercalation, or major/minor groove interactions. The difference in affinity of redox molecules to ssDNA probe and dsDNA leads to variation in the electrochemical signal before and after hybridization. This strategy is less sensitive and specific than the two former mentioned mechanisms.[66]

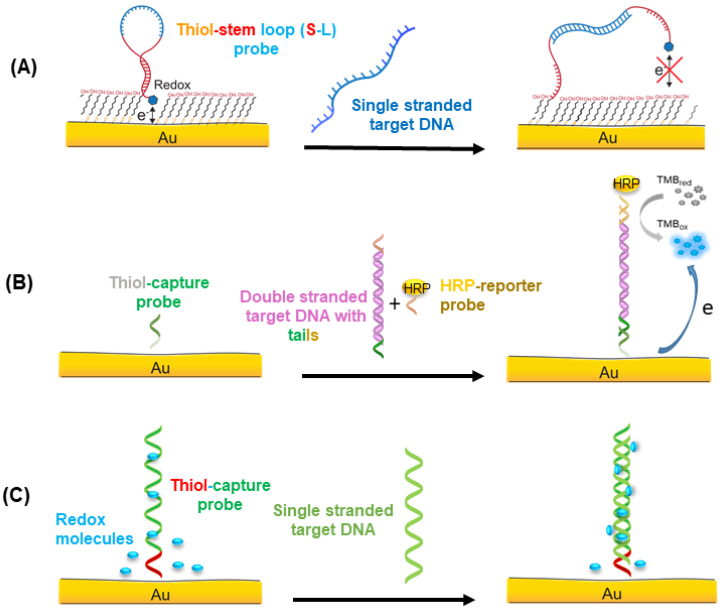

Figure 8. Illustrations of electrochemical hybridization (sequence-specific)- based DNA probes. (A) Stem-loop DNA probe functions based on the conformational change of the redox molecule-labeled probe upon hybridization of a target ssDNA. (B) Sandwich hybridization assay, in which immobilized capture probe and enzyme-labeled reporter probe detects tailed- target dsDNA in a two-step hybridization event. (C) Intercalation-based DNA probe works based on the affinity of free redox molecules to the single stranded-immobilized probe and formed dsDNA after the hybridization event.

2.5.1 Fabrication of paper/textile-based electrochemical DNA sensors for POC NAATs

Carbon is a popular electrode material in electroanalytical µPADs and µTADs because it is widely available, has high electron transfer rates, and can be easily printed on paper and textile substrates, see Figure 9.[68,69] Printed carbon pastes and inks, however, are not desirable electrodes for developing electrochemical DNA biosensors, as they generally require laborious multiple steps of functionalization that can affect the biosensors´ sensitivity and reproducibility. [67 70] Alternatively, gold is an excellent electrode that allows surface functionalization in one simple step by forming self-assembled monolayers of alkane thiol-modified DNA probes. [71]

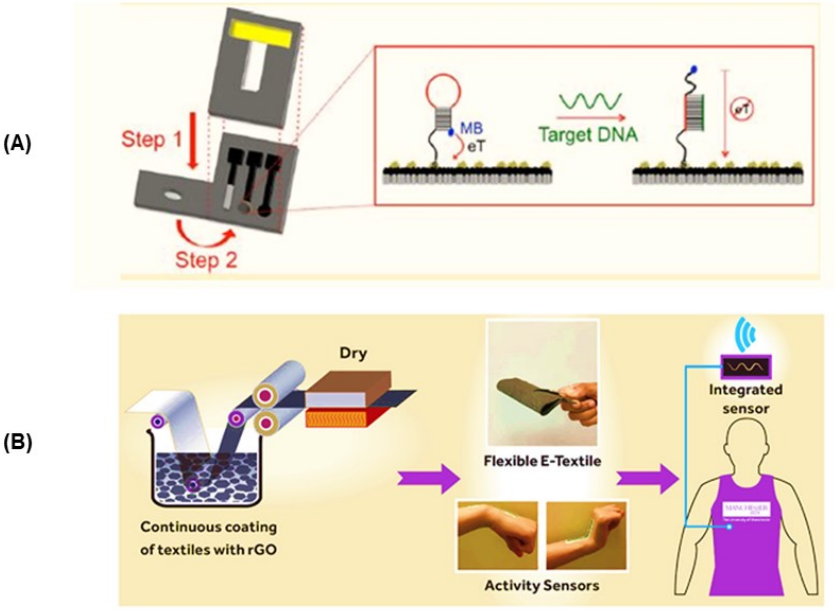

Figure 9. Electroanalytical (A) Paper-based microfluidic device (Reproduced with permission from Reference [68]. © 2014 American Chemical Society) and (B) Textile-based microfluidic device (Reproduced with permission from Reference [69]. © 2017 American Chemical Society) using printed carbon electrodes on paper and textile substrates, respectively.

Self-assembled monolayers are chemisorbed molecules with thiol, phosphate, or silane reactive groups that spontaneously form on metal substrates such as gold, silver, platinum, and cooper, see Figure 10 A. Gold surface is the most suitable substrate for thiol-SAM formation due to its high affinity and reactivity to alkanethiol molecules. [72] Gold is also biocompatible, inert, and can endure harsh chemical cleaning procedures required for sulfur-gold interaction to avoid metal-metal bonds becoming reversible after the formation of the thiolate-metal complex. This can lead to the formation of vacancy islands on the SAM functionalized surface that may affect the sensor performance and reproducibility. [73] Gold is furthermore an excellent conductor and perfect electrode for electroanalytical measurements.

Gold fiber electrodes, including gold microwires and gold threads, are suitable microscale electrodes that can be easily *ex-situ* modified with thiol-SAM DNA probes and integrated into microfluidic paper-based and thread-

based NAATs. Gold microwires (bondwires) are available at various diameters (0.0125-2 mm) with high purity (99.95-99.99%) that can be chemically or electrochemically cleaned before the formation of the SAM-DNA probe, see Figure 10 B. [74,75] Gold plasma-coated multifilament PET threads are commercially available conductive threads that can be functionalized with thiol-SAMs, without the need for pre-cleaning steps.[28] This property makes these flexible, off-the-shelf conductive threads an ideal candidate for at scale fabrication of microfluidic POC biosensors (see Figure 10 C)[28], which eliminates the need for in-house, time-consuming, usually irreproducible gold deposition on textile substrates. [76] Likewise, silver plasma-coated multifilament PET threads are also commercially available and ready to use in analytical applications.

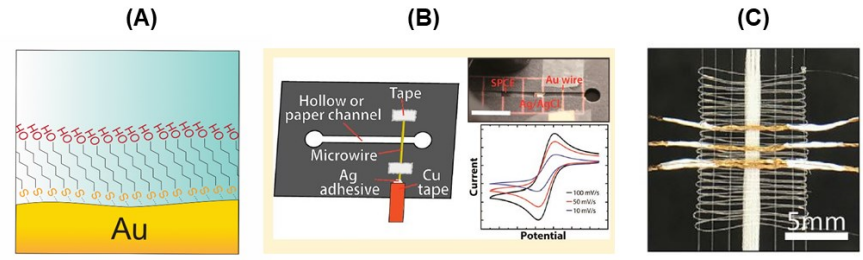

Figure 10. Gold electrodes (A) Illustration of self-assembled monolayer formation of 6-Mercapto-1-hexanol (6-MCH) on a gold surface. (Figure from **PAPER III**) (B) Integrated a gold microwire (bondwire) in a paper-based microfluidic device. Reproduced with permission from Reference [74]. © 2014 American Chemical Society. (C) Woven gold plasma coated multifilament threads in a microfluidic thread-based electroanalytical device. Reproduced with permission from Reference [28]. © 2020 WILEY-VCH Verlag GmbH & Co. KGaA, Weinheim.

3 Experimental Techniques and rationale

3.1 Samples

We used two unicellular microorganisms, *Staphylococcus epidermidis* ATCC 12228 (**PAPER I-III**) and the microalgae *Ostreopsis cf. ovata* IRTA-SMM-16-133 (**PAPER IV**) as detection targets.

Although *S. epidermidis* is among commensals and normal microbial inhabitants of the skin surface, some strains of that can cause serious infections in immunocompromised patients and nosocomial infections by forming biofilms on implanted plastic devices like dialysis catheters.[77] Thus, its diagnosis is of medical importance. In addition, *S. epidermidis* has been used as a model organism for methicillin-resistant *Staphylococcus aureus* (MRSA). MRSA can cause serious infections, including bone, joint and bloodstream infections, as well as pneumonia, and intestinal problems.[78]

The *O. cf. ovata* is known as toxic microalgae in particular Mediterranean coasts and also other temperate and tropical areas that can cause ecological, economic, and health issues such as respiratory problems, rhinorrhoea, cough, fever, dermatitis, and sometimes neutrophilia, in people subjected to marine aerosol or directly to seawater.[79] Microalgae strains of *O. cf. ova*ta (GenBank reference: MH790463) and *O. cf. siamensis* IRTA-SMM-16-84 (GenBank reference: MH790464) were used as target and negative control (NC) strains, respectively. These strains were isolated and cultured at IRTA (Catalonia, Spain). The extracted and purified genomic DNA (gDNA) of these strains were kindly provided by IRTA. The target synthetic sequence of *O. cf. ovata* was purchased from biomers.net (Germany).

3.2 Bacterial cultures, genomic DNA extraction, and purification

Lyophilized *S. epidermidis* cells ATCC 12228 purchased from ATCC LGC Standards (USA) were rehydrated with autoclaved Difco nutrient broth (234000, Becton, Dickinson and Company, MD, USA). Then, the inoculant (100-200 µL) was transferred to a cell culture flask, which contained 12-15 mL of Difco nutrient broth and incubated at 37°C overnight with shaking. Afterward, the cultured sample was used to inoculate the cells on Difco nutrient agar plates (213000, Becton, Dickinson and Company, MD, USA) at 37°C overnight. It is worth mentioning that the rest of the rehydrated cells was thoroughly mixed with medical-grade glycerol (1:1) and stored at -80°C

for long-term storage. A single colony of the cultured cells on the agar plate was transferred using an inoculation loop to the broth media at 37℃ overnight shaking. The cell pellets were collected from the cultured sample by spinning down the cultured media at 14000 xg for 10 minutes and removing the supernatant. The cultured agar plates were re-cultured according to the protocol mentioned above every month. PureLink Kit (Invitrogen, CA, USA) was used to extract the genomic DNAs from the cultured cells.

The extracted genomic DNA concentration was measured using microvolume spectrophotometers (mySPEC VWR, Sweden) and then converted to copy numbers through *Top Tip Bio online tool*, using (Equation 1):

$$Copy\ numbers = \frac{Amount\ (ng) \times 6.022 \times 10^{23}}{Length\ (bp) \times\ 10^{9} \times 650\ \left(\frac{g}{mol}\right)} \qquad \text{(Equation 1)}$$

3.3 Isothermal DNA amplification with RPA

We used RPA as an isothermal amplification method that functions with two primers at relatively low temperatures (37-42 ℃).

TwistAmp® Basic kit (TwistDX Limited Cambridge, UK) was used to amplify target amplicons of SE-0105 gene of *S. epidermidis* in **PAPERS I-III** and *O. cf. ovata* and *O. cf. siamensis* in **PAPER IV**, as target and negative control strains, respectively, at constant 37-38 ℃ according to the manufacturer's instructions. Blank samples contained all the components of the RPA master mix except any DNA but nuclease-free water instead. The gel electrophoresis technique was used to examine the efficacy of the RPA reactions using agarose gel (2%-3%), prepared in TBE buffer (0.5M).

In **PAPERS I-III**, we designed four different pairs of primers using Primer3 output and IDT primer design tool, which were customized by Eurofins Genomics Europe Shared Services GmbH (Germany). After conducting a primer screening process, we selected a set of primers that showed higher efficiency in RPA reaction to amplify the 210 bp target amplicon of the SE-0105 gene of *S. epidermidis.*

In **PAPER I**, we amplified the target sequence of *S. epidermidis* (10^4 copies/µL) with the selected primer set. In **PAPER II and PAPER III,** we used the same primer pair, but with phosphoryl group modification at the 5´ end of the forward primer to amplify the extracted and purified gDNAs of *S. epidermidis* (10 copies/µL, 50 copies/reaction), see Table 1. The obtained unpurified RPA products had conjugated phosphoryl groups on the non-target strands that were further recognized and digested by the lambda exonuclease enzyme, see Figure 11. We examined the enzymatic digestion of the non-target strands of amplicons using the gel electrophoresis technique for unpurified RPA products before and after digesting with the lambda exonuclease enzyme. This step was done as we required target single-stranded amplicons for a stem-loop DNA probe detection assay, used in **PAPERS II and III**.

Table 1. Designed RPA forward and reverse primers, as well as stem-loop (S-L) DNA probe, negative control (non-target) and target sequences of *S. epidermidis*. (Table from **PAPER II**)

Forward-Primer	5'- phosphate-TATAGGCTTAATTATCTCTGTTTTAGGAGCTT-3'
Reverse-Primer	5'-TGATAGGCACTATCTGTAAACAACATACTAAT-3'
Stem-Loop (S-L) Probe	5'MeBlN/GCGAGGAAGCTCCGGTCAACGCTTCCTCGC/3'ThioMC3-D
Target	5'-TTTTT AAG CGT TGA CCG GAG CTT CTCTTT-3'
Non-target (control)	5'-CTTATAACCTATGTAGTATCCGTA-3'

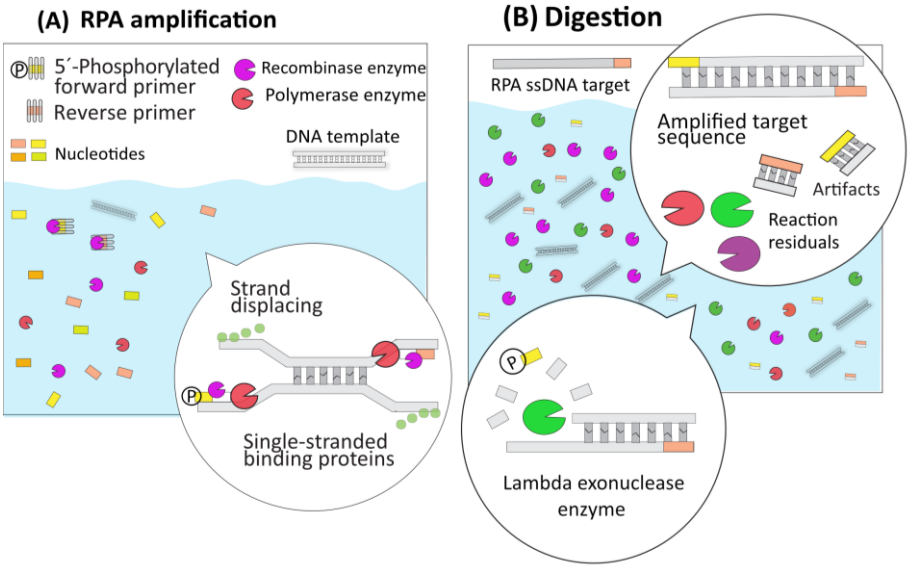

Figure 11. Illustrations of (A) The RPA reaction with a set of primers with a phosphorylated forward primer. (B) Digestion of the phosphorylated non-target strands of RPA ds-DNA by lambda exonuclease enzyme. (Figure from **PAPER II**)

In **PAPER IV**, we used a set of forward and reverse primers conjugated with oligonucleotide tails (see Table 2) customized by biomers.net (Germany) to amplify 145 bp target sequence of *O. cf. ovata* and non-target *O.* cf. *siamensis* in tube-based, and glass fiber-based RPA reactions, see Figure 12A. We freeze-dried the RPA master mix, including tailed primers, nuclease-free water, rehydration buffer of the RPA Basic Kit, and RPA enzyme pellets in glass fiber papers, which were kindly provided by Cytiva (Sweden). The RPA reactions in these substrates were initiated by rehydrating the stored components with target synthetic DNA (10 pM-0. 001 pM), target genomic DNA (1 ng/µL), non-target genomic DNA (1 ng/µL), and magnesium acetate (MgAc). These oligonucleotide tails at both strands of the amplified target sequence are designed to hybridize to capture and reporter probes in a sandwich hybridization assay (SHA), used in **PAPER IV** to detect target double-stranded amplicons, see Figure 12B.

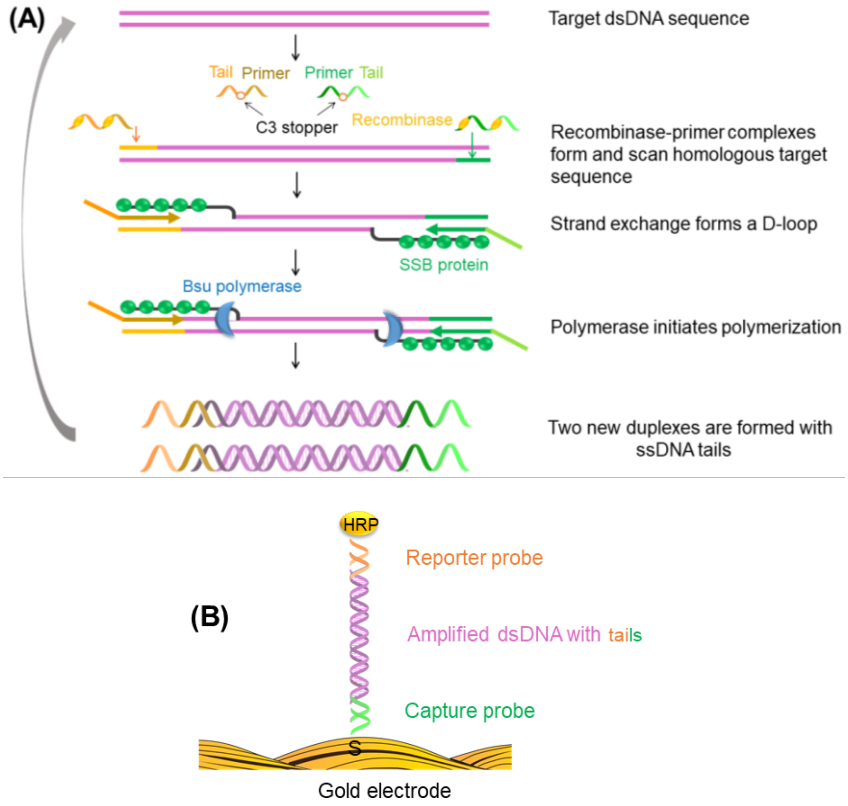

Figure 12. Illustrations of (A) The RPA reaction with oligonucleotide tail-modified primers, complementary to (B) Thiol-modified capture and HRP-modified reporter probes in the SHA assay.

Table 2. Forward and reverse primers for amplification of *O.* cf. *ovata* with C3 stopper modifications, oligonucleotide capture and reporter probe sequences and their respective modifications.

Forward-Primer with tail	5'- GTT TTC CCA GTC ACG AC-C3-ACA ATG CTC ATG CCA ATG GTG CTTGG -3'
Reverse-Primer with tail	5'-TGT AAA ACG ACG GCC AGT-C3-GCA WTT GGC TGC ACTCTT CAT ATY GT-3'
Thiolated capture probe	5'- GTC GTG ACT GGG AAA ACT TTT TTT TTT TTT TT-C3-SH-3'
HRP-labeled reporter probe	5'- HRP-ACT GGC CGT CGT TTT ACA -3'
Target	5'- ACA ATG CTC ATG CCA ATG GTG CTT GGT GGC ATG CAC CTT GTT AGT TGT AGC ATG ACA GCT TGA TAC TTA TCT AAA CGC TTT CAT CAA CTG TCT TCT GAC AGC AAT GAA TGC ATC AAT TCA AAA CAA TAT GAA GAG TGC AGC CAA ATG C -3'

3.4 Immobilization of achromopeptidase on nitrocellulose paper substrate

In **PAPER I**, we immobilized the achromopeptidase ACP (A3547, Sigma Aldrich, MO, US) on nitrocellulose (10,600,003, GE Healthcare Life Science, Germany) substrates. We conducted the RPA amplification for 10^4 copies/µL of extracted and purified genomic DNA of *S. epidermidis* in the presence of these ACP-dried nitrocellulose substrates. We investigated the effect of agitation and incubation of the ACP-treated nitrocellulose on the performance of the RPA reaction. Also, the ACP-nitrocellulose bond and the enzyme stability were studied using the gel electrophoresis technique. The obtained data were analyzed by Image Lab Software (BioRad). Also, we examined the presence of ACP enzyme in water samples, in which the nitrocellulose-bound ACP was agitated or incubated for 60 min, using the chip-based electrophoresis technique.

3.5 Experimental techniques for SAM-based electrochemical DNA sensors

3.5.1 Immobilizing DNA probes and assessing SAM formation using electrochemical techniques

We functionalized gold fiber electrodes, including gold microwires and gold plasma-coated multifilament polyester threads (see Table 3 for detailed specifications of the fiber electrodes) using thiol-modified DNA probes to fabricate sequence-specific electrochemical DNA sensors.

Table 3. Specification of the different fiber electrodes that were used in this thesis. Data are denoted as mean ± SD (n = 3).

Fiber Electrode	Yarn Number	Filament. No	Diameter (µm)	Twist type (turns/cm)	Supplier
Gold wire, 99.99% trace metals basis	-	1	100	-	SIGMA-ALDRICH
Silver wire, 99.99% trace metals basis	-	1	100	-	SIGMA-ALDRICH
Gold Plasma coated yarn Polyester FDY, high bright (1.1 mg/m Au)	dtex 125/f36/2	72	246 ± 20	5 (Z)	SWICOFIL AG
Silver Plasma coated yarn Polyester FDY, high bright (3.9 mg/m Ag)	dtex 125/f36/2	72	185 ± 19	5 (Z)	SWICOFIL AG
COOLMAX®	dtex 78/f48/4	192	896 ± 29	-	INVISTA

In **Paper II and III**, gold microwire electrodes (100 µm diameter, 99.99% trace metals basis, Sigma-Aldrich, Sweden) were first electrochemically cleaned (electropolished) in sulfuric acid solution (0.5 M) by conducting CV method in a potential window of -0.4 V to +1.350 V at a scan rate of 0.1 V/s versus Pt or Ag/Ag Cl standard reference electrode, until the cyclic voltammogram stabilized. The electropolished gold microwires were rinsed thoroughly with MQ-water and dried with nitrogen gas. Then, these clean gold microwires (0.5 cm) were functionalized with stem-loop oligonucleotide DNA probes (Integrated DNA Technologies IDT, USA) with methylene blue and disulfide (C3 S-S) modifications at 5´ and 3´ ends, respectively, see Table 1. The disulfide bonds of the stem-loop DNA probes were reduced to thiol groups using TCEP (Sigma-Aldrich, Sweden) reducing agent before incubating with the clean gold microwires. The unlabeled sites of the stem-loop probe-modified microwires were further passivated with 6-Mercapto-1-hexanol (6-MCH) (Sigma-Aldrich, Sweden) to hinder non-specific adsorption of DNA molecules in the subsequent hybridization at the detection step and also to detach the nonspecifically adsorbed DNA probes from the surface of the electrodes.[80,81]

In **PAPER IV**, we used off-the-shelf gold plasma-coated PET multifilament threads (SWICOFIL AG, Switzerland) to develop SHA, including the thiol-modified capture and HRP-conjugated reporter probe. Firstly, a geometric area of 0.5 cm length was defined on gold threads using nail polish to stop the flow of fluid to the metal connectors for further electrochemical measurements. Secondly, the gold threads were functionalized with thiol-modified capture probes without the need to clean the electrodes beforehand.

The CV technique was used to examine the formation of thiol-SAM DNA probes on the surface of gold microwires and gold threads electrodes.

In **PAPER II** and **PAPER III**, the formation of SAM of stem-loop DNA probe on the gold microwires were investigated by CV (potential window of -0.2 V to +0.2 V and at 0.05 V/s scan), and SWV for -0.05 V and +0.15 V at 50 Hz frequency and amplitude of 0.02 V and a step potential of 0.01 V. We used a three-microwire electrode setup including a stem-loop DNA probe modified gold microwire, a silver microwire (100 µm diameter, 99.99% trace metals basis), and two gold microwires as working, pseudo reference, and counter electrodes, respectively. The coverage or density of stem-loop DNA probe on the modified gold microwires was calculated using the charge under the

methylene blue oxidation peak in CVs collected for three individual electrochemical DNA (E-DNA) sensors at scan rates of 0.05 V/s, 0.02 V/s, and 0.01 V/s scan rate, using (Equation 2):

$$\Gamma = Q/nFA \qquad \text{(Equation 2)}$$

Here surface density of the probe is Γ (molecules/cm^2), the amount of charge is Q (coulombs) transferred in cyclic voltammograms of the redox molecule, the number of transferred electrons is n=2 for MB molecules. Faraday´s constant and electroactive surface area (cm^2) of the electropolished gold microwires are shown by F and A, respectively.

We examined the formation of SAM on the capture probe-modified gold threads in **PAPER IV** and that of 6-MCH-modified gold microwires and gold threads in **PAPER III** using the CV method in 5 mM of K_3 Fe $(CN)_6$ solution (Sigma Aldrich, Sweden) versus silver microwire/thread pseudo reference electrodes at a scan rate of 0.05 V/sec in a potential window of -0.1V to +0.45V.

Randles–Sevcik equation (Equation 3) was used to calculate the effective surface area of unmodified and 6-MCH-modified gold microwires and threads, as well as that of the gold threads before and after immobilization of the capture probe on the electrode surfaces. We used the slope of the *ip* versus $v^{1/2}$ plot obtained by CVs at 0.01-0.3 V/s scan rates.

$$i_p = (2.69 \times 10^5)\, n^{3/2} D^{1/2} C A v^{1/2} \qquad \text{(Equation 3)}$$

Here the number of the electron involved in the redox reaction is n=1, see (Equation 4), the diffusion coefficient (D) and the molar concentration of the redox solution (C) are 6.70×10^{-6} cm^2/s and 5×10^{-6} mol/cm^3, respectively. The scan rate and the electrochemical effective surface area are shown by v (V/s) *and* A (cm^2), respectively.

$$[Fe(CN)_6]^{3-} + e^- \rightleftharpoons [Fe(CN)_6]^{4-} \qquad \text{(Equation 4)}$$

3.6 The SAM-based electrochemical assays used in this thesis

In this thesis, we used two different sequence-specific, thiolated-DNA probe structures and assays, including the stem-loop DNA probe and sandwich hybridization assays in combination with the RPA method for POC NAATs. The main difference between these two assays was that the stem-loop DNA probe was representative of a redox-labeled sequence-specific DNA probe that forms redox-active SAM on gold electrodes, while SHA assay exploited a label-free SAM assay. The electrochemical responses of the fabricated fiber-based DNA sensors were statistically analyzed using the Student's t-test.

3.6.1 Stem-loop probe electrochemical DNA (E-DNA) sensor

In **PAPER II** and **PAPER III**, we used the stem-loop probe assay built on the initial work of the Plaxco group [82] to detect the RPA amplified target of *S.epidermidis* pathogen. The assay is based on the stem-loop shape DNA probe with a conjugated redox-active molecule (we used methylene blue, MB). This probe has a double-stranded oligonucleotide stem with a single-stranded oligonucleotide loop, complementary to the target sequence, see Figure 13. In the absence of the target, the redox tag (MB) is in close vicinity of the electrode leading to efficient electron transfer between the redox molecule and surface of the electrode. Hybridization of the target sequence to its complementary loop part of the probe, however, opens the loop and changes the position of the redox probe. This conformational change results in a lower redox activity that is measured by sensitive electrochemical techniques such as SWV (described in *section 2.5*), which shows suppressed current peak after hybridization of the target sequence with the DNA probe compared to a baseline peak current in the presence of a pure PBS (1X) solution.

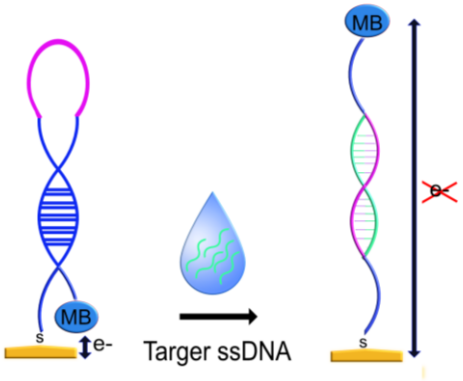

Figure 13. Illustration of the methylene blue (MB)-modified stem-loop DNA probe immobilized on a gold surface through thiol chemistry.

The responses of microwire E-DNA sensors were calculated based on the current peak suppression of SWV scans using (Equation 5) for three independent sensors after 5-20 minutes of incubation with target synthetic DNA (0.2 – 8 µM), unpurified digested RPA target, and blank samples.

$$Signal\ Suppression\ (SS) = (\Delta Ib - \Delta Iss/\Delta Ib) \qquad \text{(Equation 5)}$$

Where ΔIb is the current peak baseline (in PBS (1X)) and ΔIss is the recorded SWV current after incubation with the RPA target or blank samples. Before calculating the signal suppression, all recorded peak currents were normalized to the lowest recorded current in the corresponding SWV scans. The technical limit of detection of the E-DNA sensors was determined based on three standard deviations (SD) of average signal suppression of blank samples divided by the slope of the linear calibration plot (0.2-1µM) of the target synthetic sequence.

3.6.2 Sandwich hybridization assay (SHA) electrochemical DNA sensor

In **PAPER IV**, we fabricated a sandwich hybridization assay electrochemical DNA sensor using thread electrodes. The sensor performance was characterized with the RPA products of target *O.* cf. *ovata* and non-target *O.*

cf. siamensis microalgae strains. Unlike the stem-loop E-DNA assay, the SHA assay benefits from two different DNA probes (thiol-capture and HRP-labeled-reporter probes) to capture and report the target dsDNA sequence. Therefore, this SHA assay eliminates the need for digestion of RPA products before the detection step due to the tailed-RPA products. These two SHA probes are complementary to the tails of the RPA target products. The SHA assay provides electrical signals in the presence of the target, based on the enzymatic reaction between the HRP enzyme (conjugated to the reporter probe) and TMB+H_2O_2 substrates by applying a reduction potential of -0.1 V to the working thread electrodes, see Figure 14. After 5 minutes of incubation with the substrate, currents were recorded at 1 second.

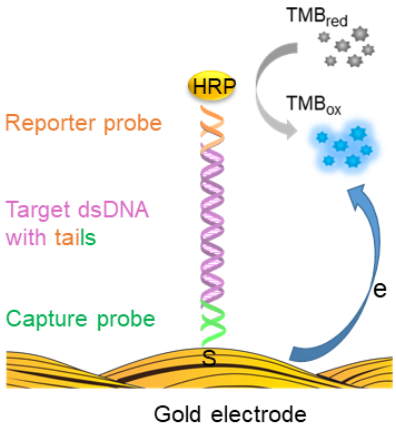

Figure 14. Illustration of the sandwich hybridization assay (SHA) for detecting target dsDNA using a thiol-capture probe immobilized on a gold fiber electrode and an HRP-modified reporter probe.

3.7 Integrating fiber SAM-based electrochemical DNA sensors into microfluidic paper and textile devices

3.7.1 Woven stem-loop DNA probe E-DNA sensor

In **PAPER III**, we integrated the microwire-based stem-loop E-DNA sensor into a woven microfluidic device fabricated using a portable weaving loom. This woven microfluidic device was structured by weaving eight Coolmax® yarns (Invista, UK) as horizontal wicking channels, such that each of the microwire electrodes was sandwiched between two Coolmax® yarns. The integrated three-electrode setup consisted of the SAM-modified gold microwire, silver microwire, and two gold microwires as working, pseudo

reference, and counter electrodes, respectively. Also, three Coolmax® wicking channels (three yarns/channel) were vertically weaved to the integrated fiber electrodes. Finally, the woven device was framed by weaving five strands of cotton yarns to the top and bottom of the weave, see Figure 15.

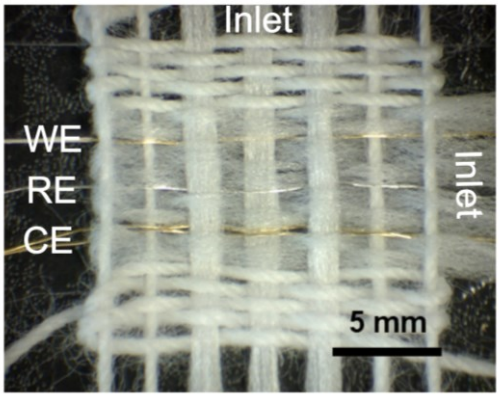

Figure 15. Photo of the Coolmax®-cotton woven device with integrated fiber electrodes including gold working (WE), silver pseudo reference (RE) and two gold counter (CE) microwire electrodes. (Figure from **PAPER III**)

The woven stem-loop E-DNA sensors were characterized by loading unpurified, digested, and diluted RPA products, including RPA target and blank samples, into the Coolmax® inlets of the device. We conducted CV at -0.2V to +0.2V potential window, at 0.05 V/s scan rate and SWV with 0.01 V potential step, 0.02 V amplitude, and 70 Hz frequency for three-times, after 5 minutes of incubation with the samples. The responses of the woven E-DNA sensor were calculated using (Equation 5).

Also, the unmodified and 6-MCH-modified gold microwires and threads were electrochemically characterized in three sequential steps, before weaving, in the weave, and after removing them from the weave by conducting the CV in the presence of 5 mM of potassium ferricyanide redox solution at different scan rates of 0.01-0.3V/s. In these measurements, gold and silver microwires/threads were used as counter and pseudo reference electrodes, respectively. The electrochemical performance of the unmodified and 6-MCH-modified gold fiber electrodes in the conditions mentioned above were investigated using corresponding CVs and Randles–Sevcik (Equation 3).

3.7.2 Flexibility Characterization of woven fiber electrodes

In **PAPER III**, the electrochemical performance of the integrated thread and microwire electrodes into the woven devices were characterized using the CV technique in three different forms, including straight, 90 degree-bend, and folded form, as they were attached to a finger of a human subject. The current densities of both woven fiber electrodes in these three conditions were calculated by dividing oxidation peak currents of potassium ferricyanide redox solution (5 mM) in CVs to the electrochemical effective surface area of either of the fiber-electrodes.

3.7.3 Scanning Electron Microscope (SEM)

In **PAPER III**, the scanning electron microscope (SEM) technique was used to study the topography of the off-the-shelf plasma-coated gold and silver threads as well as the electropolished gold microwires, using a Hitachi Tabletop SEM TM-1000 (Japan).

3.7.4 Paper-based electrochemical SHA sensor

In **PAPER IV**, we integrated the electrochemical thread-based SHA assay into a 3D paper-based electrochemical DNA sensor to detect the RPA amplified target of *O.* cf. *ovata*. The paper-based device consisted of 7 layers, including a glass fiber pad and different layers of Whatman filter paper Grade 1 with 5 mm width-hallow or filter paper channel defined by the wax printing technique. Figure 16 illustrates these different layers: (1) a wax layer with a hollow channel, where the capture probe-modified gold thread (the working electrode) was located; (2) a wax layer with a filter paper channel, in which the RPA sample is incubated with the working thread electrode; (3) a plain wax layer with a flange (the first blocking layer), which isolates and holds the sample at the incubation step; (4) a glass fiber absorbent pad was used to absorb the samples and Milli-Q water at the rinsing step; (5) a plain wax layer with a flange (the second blocking layer), which prevents leaking of the fluid from absorbent layer to underneath detection layers; (6) a wax layer with hallow channel was used as a spacer; and (7) a wax layer with filter paper channel served as detection layer, in which a silver thread and two gold threads (0.5 cm length) were placed as a pseudo reference and counter electrodes, respectively. Layers 2, 4, and 5 were taped together as a removable absorbent layer. These seven layers were aligned with double-sided tape and laminated between two plastic substrates.

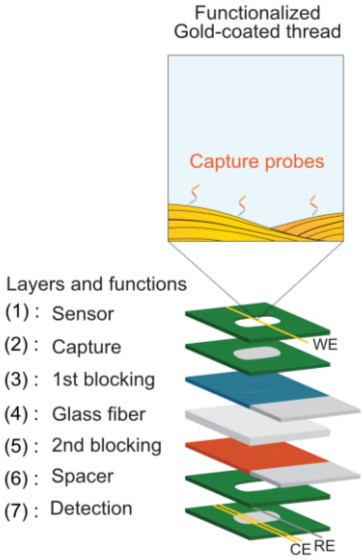

Figure 16. Illustration of the different layers and their functions in the paper-based electrochemical SHA DNA biosensor. (Figure from **PAPER IV**)

The paper-based SHA DNA sensors were characterized by adding pre-incubated RPA products (tube-based purified or freeze-dried based unpurified RPA samples) with the HRP labeled-reporter probes to the inlet of the device. This paper-based assay was followed by subsequent incubation, rinsing, and detection steps included in the device, simply by removing blocking wax layers and removable absorbent layer at different steps. The chronoamperometric measurements were conducted by connecting the integrated three-thread electrode setup to an Autolab potentiostat (PGSTAT204N Metrohm Autolab, Sweden) in the presence of TMB+H_2O_2 enzymatic substrate, waiting for 5 minutes, applying the reduction potential of -0.1 V, and recording the output current at 1 second. The limit of detection (LOD) in this assay was determined based on the mean of the non-target strain plus three times SD using the calibration curve (for10 pM-0.001 pM target synthetic DNA) fitted using Origin 9.1 software.

4 Results and discussion

This thesis aimed to investigate and demonstrate the applications of fiber materials, including paper, threads, and microwires, as potential and suitable candidates for fabricating electroanalytical POC diagnostics (e.g., NAATs). First, this section will introduce rationales and methods for some experiments and then present and discuss the main results divided into three main steps of NAATs: sample preparation, nucleic acid amplification, and detection.

4.1 Sample preparation using nitrocellulose paper

Sample preparation is the limiting step in POC NAATs, as it necessitates multistep of manual intervention and instrumentations. Sample preparation includes cell lysis for nucleic acid extraction and purification, which commonly utilize chemicals or enzymes. Peptidases are a group of enzymes, including proteinase K, papain, and acid phosphatase enzymes (ACP).[83] These enzymes catalyze the hydrolysis of proteins and are therefore widely used to digest cells and tissues. [84] ACP is specifically reported as an effective mixture of enzymes that lyses Gram-positive bacteria, which are hard to lyse due to their thick cell wall. [85] Enzymes, however, need to be deactivated, as they can inhibit or interfere with the downstream NAATs steps such as nucleic acid amplification and detection. For instance, ACP requires heat deactivation at 80 °C or multiple steps of washing for its removal from the reaction media. [86] These steps are not compatible with microfluidic POC applications. [87] To address these obstacles, in **PAPER I**, we investigated the possibility of using nitrocellulose paper, which has a long history in Western blot analysis [88] and paper-based immunoassay,[89] for immobilizing the ACP enzyme. We examined the effect of nitrocellulose-bound ACP on the isothermal amplification of genomic *S. epidermidis* (10^4 copies/µL) through the RPA method, see Figure 17.

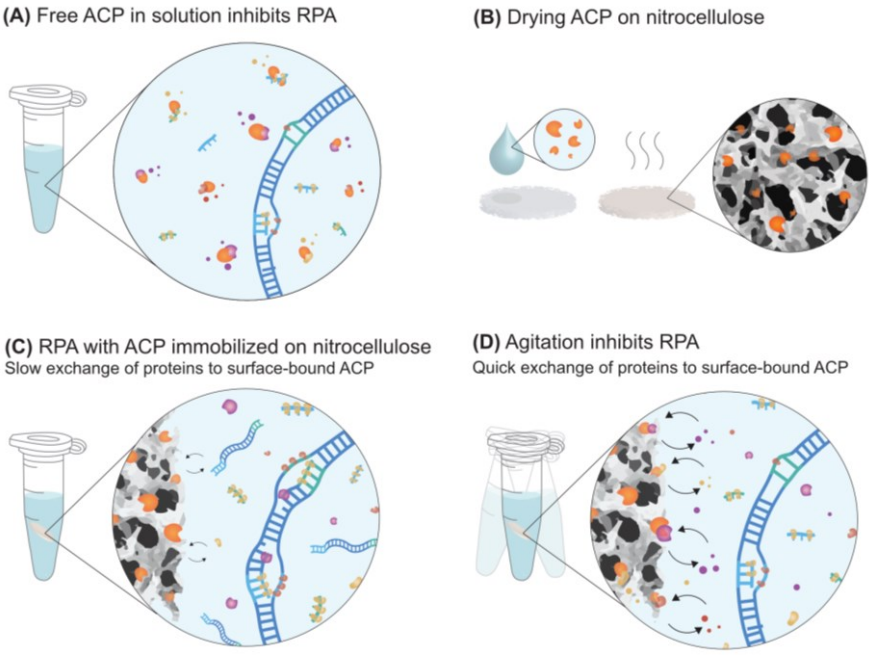

Figure 17. Illustration of the RPA reaction in the presence of ACP enzyme(A) Free ACP enzyme in the RPA reaction may digest other enzymes involved in the amplification. (B) ACP is air-dried on the nitrocellulose substrate. (C) The RPA reaction is not inhibited instantly by undisturbed ACP-treated nitrocellulose membranes. (D) Agitating the ACP-treated nitrocellulose in the RPA reaction may enhance the rate of reagent exchange at the substrate-solution interface. (Figure from **PAPER I**)

The densitometric analysis of gel electrophoresis of RPA products revealed that unlike ACP in solution (see Figure 18 A), the undisturbed ACP on nitrocellulose does not immediately inhibit the RPA reaction shown in Figures 17 A and 17 C, respectively. The agitated or incubated (for 60 minutes at room temperature) nitrocellulose-bound ACP in the RPA master mix, however, remarkably diminished the performance of the RPA reaction, as there was no statistically significant difference between these and negative control samples, which contained nuclease-free water in the RPA master mix instead of any DNA templates, see Figures 18 C and 18 D.

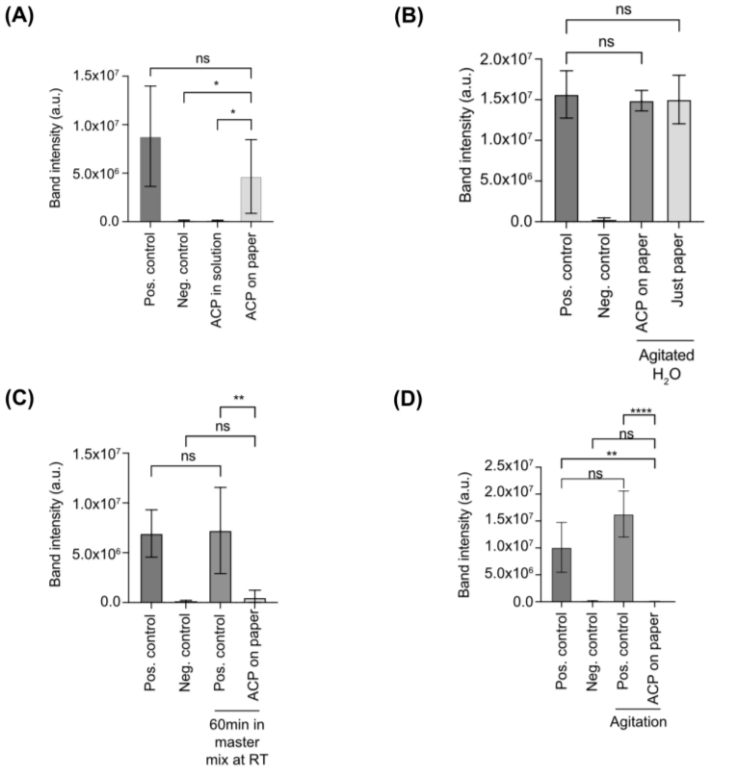

Figure 18. Calculated target band intensity of RPA products in the presence of the ACP-treated nitrocellulose using electrophoresis images. (A) Unlike ACP in solution, the RPA reaction was not notably influenced by undisturbed ACP-treated nitrocelluloses. (B) The RPA reaction was not inhibited remarkably in the presence of water samples, in which the ACP- treated nitrocelluloses or plain nitrocelluloses were agitated. (C) ACP-treated nitrocellulose inhibited the RPA reaction after 60 minutes of incubation at room temperature. (D) Agitated ACP-treated nitrocellulose inhibited the RPA reaction. Data are shown in mean with SD for n = 5 for all conditions. Unpaired t-test, ns: not significant ($P \geq 0.05$), * significant at $p \leq 0.05$, ** significant at $p \leq 0.01$, **** significant at $p \leq 0.0001$, (Figure from **PAPER I**)

To investigate the ACP-nitrocellulose bond and the enzyme stability on nitrocellulose substrate, we agitated or incubated the ACP-treated nitrocellulose paper in nuclease-free water samples and added the spiked water into the RPA reaction. We analyzed the spiked water samples using the chip-based electrophoresis technique. The intensity of the target band (at

210 bp) of RPA products that contained the spiked water samples in their master mix was quantified in their corresponding gel electrophoresis images. The gel image of the chip-based electrophoresis shown in Figure 19 indicated the ACP bands (30-50 kDa) for free ACP in water samples, while they were absent for both agitated and incubated ACP-treated nitrocellulose in the corresponding water samples. The densitometric analysis of the gel electrophoresis image of RPA products showed successful RPA reactions in the presence of these spiked water samples, see Figure 18B. These were inconsistent with the quantified gel electrophorese results shown in Figures 18C and 18D that indicated inhibited RPA amplification reactions for the agitated or incubated RPA reaction, for 60 minutes at room temperature, in the presence of ACP-treated nitrocellulose paper. These findings reveal that, although ACP does not easily diffuse or release to the RPA reaction, it can inhibit the RPA function if the reaction is disturbed by agitating or incubating for an hour at room temperature. We hypothesized that in the two latter conditions, the RPA enzymes (recombinase and polymerase) diffuse and interact with the immobilized ACP at the nitrocellulose-solution interface, leading to the deactivation of the RPA enzymes and failure of the amplification.

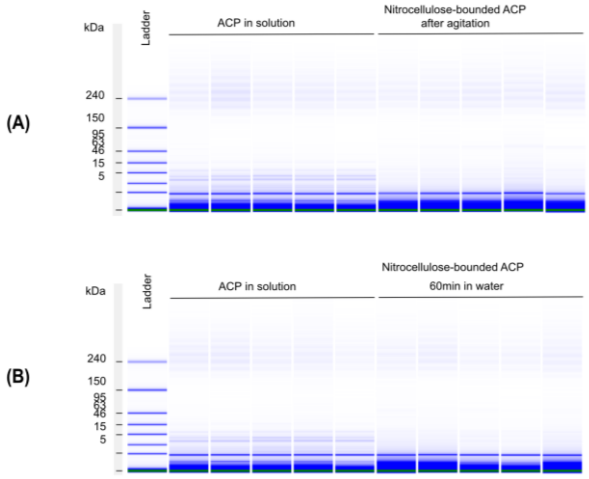

Figure 19. Gel electrophoresis images of chip-based electrophoresis of free ACP in solution (30 to 50 kDa) and water samples in which (A) Nitrocellulose-bound ACP was incubated for 60 min. (B) Nitrocellulose-bound ACP was agitated. (Figure from **PAPER I**)

This study showed the potential of using ACP-treated nitrocellulose for the sample preparation in POC NAATs. This method eliminates the need for heat-deactivation of enzyme and washing steps (which require instruments and laborious manual intervention) since ACP can be easily removed from the solution by removing the nitrocellulose. Thus, it facilitates the integration of sample preparations in microfluidic POC NAATs.

4.2 Fiber-based electrochemical DNA sensors

Fiber substrates like textiles and papers cannot easily incorporate gold electrodes using common techniques (e.g., printing), especially for fabricating SAM-based biosensors that require clean and pure gold surfaces for thiol chemistry-based functionalization. Fabrication of gold threads in these porous materials generally requires multistep of in-house fabrication, which is generally tedious, expensive, and not applicable at scale.

In this thesis, we have solved this problem by using gold microwires (bondwires) and gold plasma-coated PET multifilament threads. These gold microelectrodes, along with their silver counterparts, are commercially available on spools (see Figure 20) that enable the fabrication of electrochemical DNA biosensors for NAATs with the potential of miniaturization into POC μPADs and μTADs.

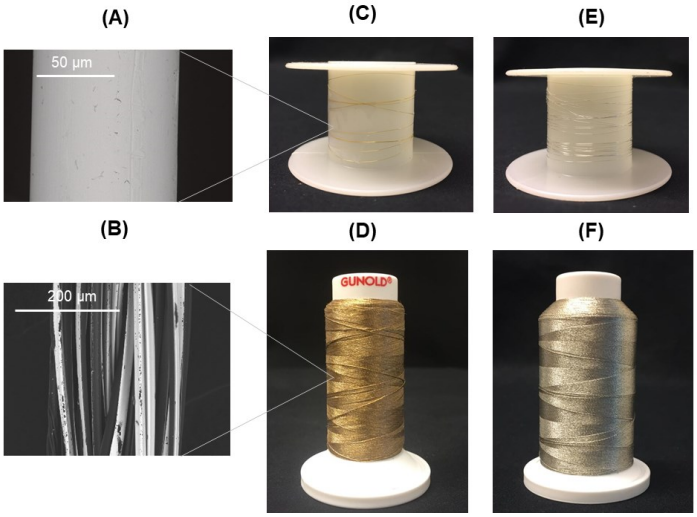

Figure 20. Scanning electron microscope (SEM) images of (A) Gold microwires and (B) Gold plasma-coated PET multifilament threads. Photos of a spool of (C) Gold microwires (bondwires) and (D) Gold threads. Photos of a spool of (E) Silver microwires and (F) Silver plasma-coated PET multifilament threads.

4.3 Integrating RPA and stem-loop probes in a minimal DNA assay

One of the initial works in **PAPER II** was to develop an assay that could combine the RPA method for isothermal amplification of genomic DNA of *S. epidermidis* with stem-loop DNA probe, as this had not been reported before to the best of our knowledge.

The main idea was to design a stem-loop probe, fabricate a SAM-based DNA biosensor on the clean gold microwires (0.1 mm diameter), and subsequently use the amplicons from RPA reactions to characterize the fabricated fiber-based electrochemical sensor. To perform the stem-loop DNA probe detection, however, target double-stranded amplicons had to be converted into single strands. To achieve this, we used the lambda exonuclease enzyme, a highly processive 5'→3' exodeoxyribonuclease that selectively digests the 5'-phosphorylated strand of dsDNA.[90]

We first characterized the performance of the stem-loop probe E-DNA sensors using target and negative control synthetic ssDNA (4 μM) by SWV method, see Figure 21A. The calibration plot of the biosensor shown in Figure 21B was obtained in the presence of 0.2-8 μM of target synthetic ssDNA. The E-DNA sensors showed a linear response in a range of (0.2-1 μM) that accordingly determined the technical LOD of 0.5 μM (see *experimental 3.6.1*). Then, we examined the E-DNA sensors with unpurified diluted (500-fold) RPA products for the target genomic DNA of *S. epidermidis* (10 copies/μL) and blank samples, which contained nuclease-free water instead of DNA templates in the PRA master mix. Both samples were treated with the lambda exonuclease enzyme (see Figure 21 C), which selectively digested the 5´-phosphorylated-non-target strand of the amplicons provided by the phosphorylated-forward primer at 5´ ends during the RPA reaction. The digested target amplicon (210 bp) migrated further and emerged at a lower band than dsDNA in the agarose gel. This could be due to the higher electrophoretic mobility of the ssDNA than that of the dsDNA.[52] Three examined independent E-DNA sensors indicated a statistically significant difference between the target and blank samples of RPA after 5 and 10 minutes of incubation, see Figure 21 D. For longer periods of incubation of 15 and 20 minutes, however, the E-DNA sensors could no longer discriminate the target samples statistically. This might be due to the fouling of the electrodes. Biofouling of biosensors arises from nonspecific adsorption or adhesion of biomolecules present in samples (e.g., proteins) throughout the assay.

The results showed that the stem-loop probe could specifically bind to the target ssDNA. Moreover, this binding event would occur even in the presence of residual by-products from the RPA reaction.

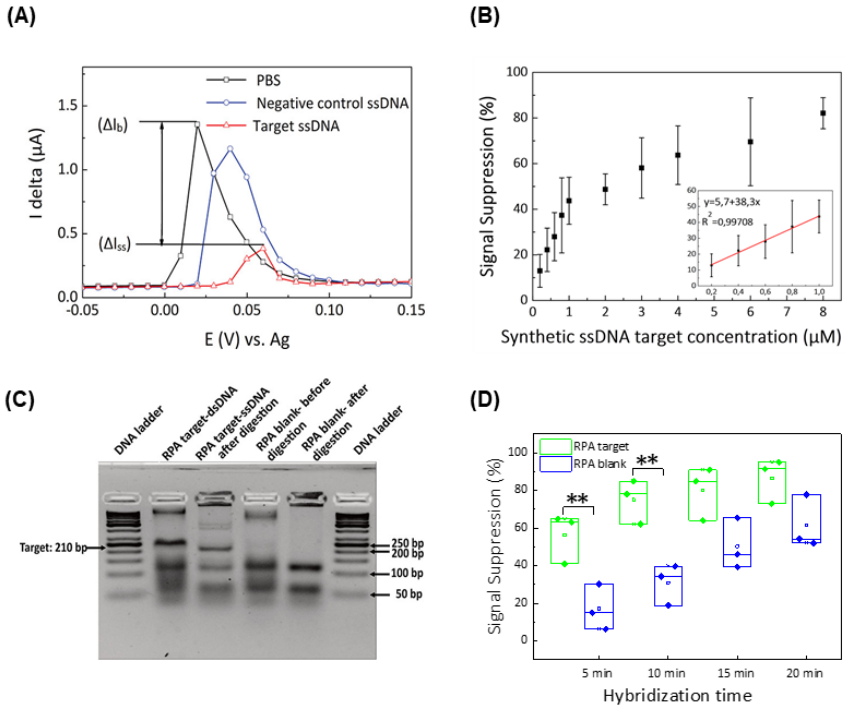

Figure 21. Characterization of microwire-based E-DNA sensors (A) SWV responses of E-DNA sensors in the presence of target and negative control synthetic ssDNA (4 μM). (B) Calibration plot of E-DNA sensors (n=3) using target synthetic ssDNA. (C) Gel electrophoresis of RPA products of *S. epidermidis* gDNA (10 copies/μL) and blank samples before and after digesting with lambda exonuclease enzyme (D) Electrochemical responses of E-DNA sensors (n=3) in the presence of unpurified, digested RPA products (ssDNA) based on the signal suppressions in their corresponding SWV measurements. ** significant at $p \leq 0.05$. (Figure from **PAPER II**)

Even though the DNA digestion and dilution steps added two more steps to the assay, the presented microwire-based stem-loop E-DNA sensors offer: (1) a quick response time, in less than 15 minutes; (2) a specific detection of unpurified RPA products, which eliminates the need for purification steps after the RPA amplification; (3) a sensitive assay that in combination with RPA method provide a LOD of 10 copies/μL of genomic DNA of *S. epidermidis*; and (4) a total assay time of 70-75 minutes, from RPA amplification to electrochemical detection.

4.4 Integrated fiber-based micro total analysis systems (µTAS)

Once we had established the RPA and the stem-loop DNA probe assay, we proceeded to integrate this assay into a fiber-based microfluidic system, using textiles as a platform for µTAS systems.

4.4.1 Woven µTAS

Threads and yarns feature inherent 3D structure and wicking property that enable cleanroom-free microfabrication of the microfluidic devices for POC diagnostics, without the need for external pumps to flow liquids in the system.

Weaving as a bottom-up approach can achieve different structures of basic building blocks for textile microfluidics, using Coolmax® yarns in combination with conducting threads, acting as electrodes.

To achieve microfluidic properties, we focused on the commercial Coolmax® fibers. These fibers were originally designed by DuPont for sportswear to transport sweat efficiently away from the body inside its grooved channels, see Figures 22 C and 22 D as well as Figures 23 A and 23 B.

Previously, our group studied the wicking properties of Coolmax® yarns with different wicking channels, including the Ne 24/2 Coolmax® with four wicking channels (tetrachannel), the dtex78/f48/2 and dtex78/f48/4 Coolmax® yarns with six channels, along their length (hexachannel), see Figures 22C and 22D.[28] The distance that the methylene blue dye in water solution wicked versus the test time showed that the dye molecules in Coolmax® yarns with hexachannel (dtex78/f48/2 and dtex78/f48/4 yarns) wicked faster and longer distances than the one with tetrachannel shapes (Ne 24/2), see Figure 22 A. Figure 22 B indicates the plotted wicking distance versus square root of time, also confirmed that the flow of the fluid in these examined Coolmax® yarns followed the Washburn equation (Equation 6).[91]

$$L = \sqrt{\frac{\gamma r t \cos\theta}{2\eta}} \qquad \text{(Equation 6)}$$

Where L is the penetration distance, γ is the surface tension, r is the average pore radius, θ is the contact angle between the fluid and the solid substrate (capillary wall), t is the time course, and η is the dynamic viscosity of the liquid.

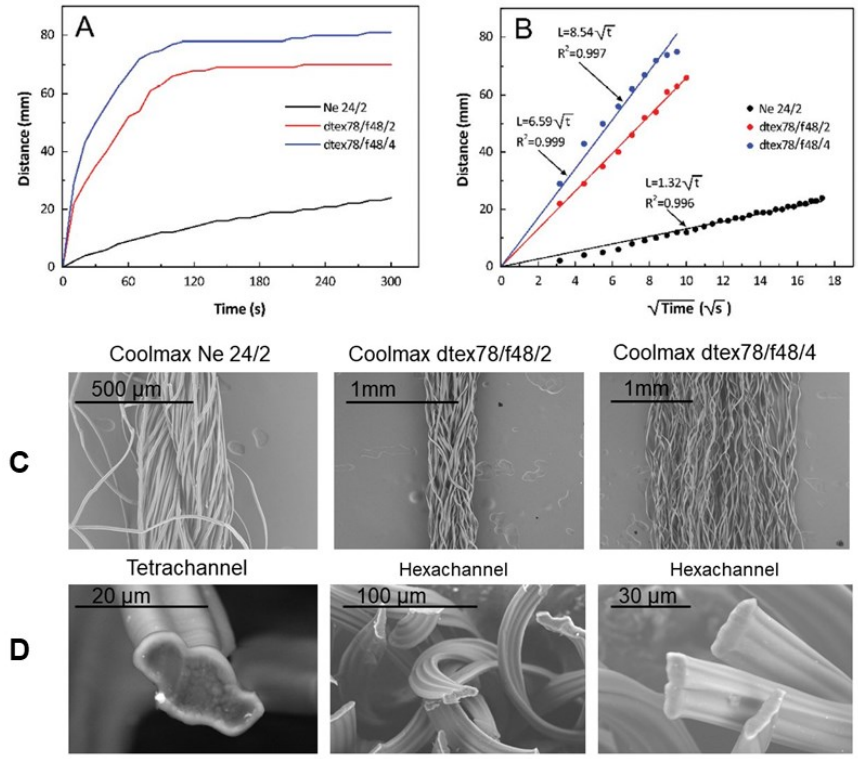

Figure 22. Characterization of wicking behavior of three different Coolmax® yarns (A) The distance that the methylene blue dye in water solution wicked through the fibers versus the test. (B) Washburn equation plots. (C) and (D) SEM images of these Coolmax® yarns from the side view and the cross-section view, respectively. Reproduced with permission from Reference [28]. © 2020 WILEY-VCH Verlag GmbH & Co. KGaA, Weinheim.

Our group also characterized the Coolmax® yarns in terms of transport of molecules, which is of interest for microfluidic fiber-based diagnostics. Three different samples models, including bovine serum albumin (BSA), ruthenium hexamine chloride (RHC), and 17 mer synthetic ssDNA, wicked across a certain length of the dtex78/f48/2 Coolmax® yarns. The results showed no constant loss of samples over the test distances, see Figures 23 (C-E). This revealed that these fibers work very well as microfluidic channels for bioanalytical assays.[28]

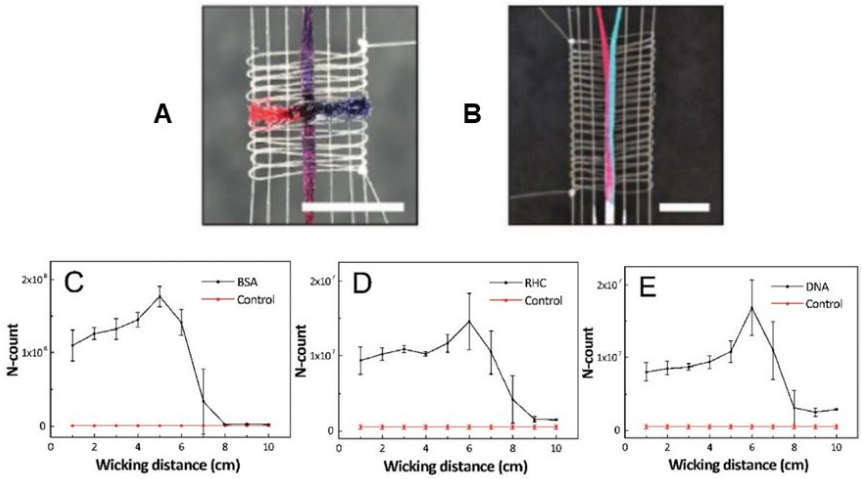

Figure 23. Photos of woven Coolmax® yarns in the (A) Perpendicular and (B) Horizontal structures for transport of different model samples; scale bars show 5mm. Concentration gradients of three model molecules, including (C) BSA protein (D) RHC redox molecules, and (E) Synthetic ssDNA, over wicking distance of Coolmax® yarns. Control lines in red indicate nitrogen content for bare Coolmax® yarn cuts. Reproduced with permission from Reference [28]. © 2020 WILEY-VCH Verlag GmbH & Co. KGaA, Weinheim.

4.4.2 Woven electrochemical DNA sensors

In **PAPER III**, we combined woven µTAS devices with the stem-loop E-DNA and RPA assay to realize a woven electronic NAAT device. We fabricated the woven electrochemical DNA sensor by weaving Coolmax® yarns as wicking channels and cotton yarns to frame the weave.

The woven microfluidic is structured by weaving the Coolmax® yarns (8 yarns) in the horizontal direction to the fiber electrodes (SAM-modified microwire/thread as working, silver microwire/thread as a pseudo reference, and two gold microwires/threads as counter electrodes, each electrode were sandwiched between two wicking channel) and three vertical Coolmax® channels (three Coolmax® yarn/channel) to the electrode. This woven structure (see Figures 24B and 24D) provided maximum liquid contact at the electrode surface and consistent flow behavior in the woven device.

We conducted a systematic study on the 6-MCH-modified clean gold microwires and off-the-shelf gold threads to examine these SAM-modified fiber electrodes' electrochemical performance and electrochemical effective surface area before weaving, in the weave and after removing from the weave. We conducted the CV technique using the three-electrode setup (with microwires or threads) in the presence of potassium ferricyanide redox solution (5 mM) at different scan rates of 0.01-0.3 V/s.

The CV scans and calculated electrochemical effective surface area of the 6-MCH-modified gold fiber electrodes, using the Randles–Sevcik equation (Equation 3), revealed that the off-the-shelf gold thread electrodes provide three times higher electroactive surface area than that of the clean gold microwires, see Table 4.

Table 4. The effective electrochemical surface area of unmodified and SAM 6-MCH-gold fiber electrodes, including gold microwires and gold threads before weaving, in the weave, and after removing from the weave. (Table from **PAPER III**)

Electrochemical effective surface area (mm^2)				
Au fiber Electrode	**Unmodified**	**6MCH-modified** Before weave	In weave	After weave
Wire	2.7± 0. 2	densely packed	densely packed	1.4 ± 0.9
Thread	7± 3.8	densely packed	3.6± 2.6	6.5± 2.7

The 6-MCH-modified gold threads, however, were more vulnerable to mechanical tensions in the weaving process than the gold microwires that could cause damage to the SAM on the electrode surface. This effect was revealed by corresponding CVs shown in Figures 24 A and 24 C. Therefore, we chose gold microwires as the working electrodes for integrating the stem-loop E-DNA sensor into the woven microfluidic device.

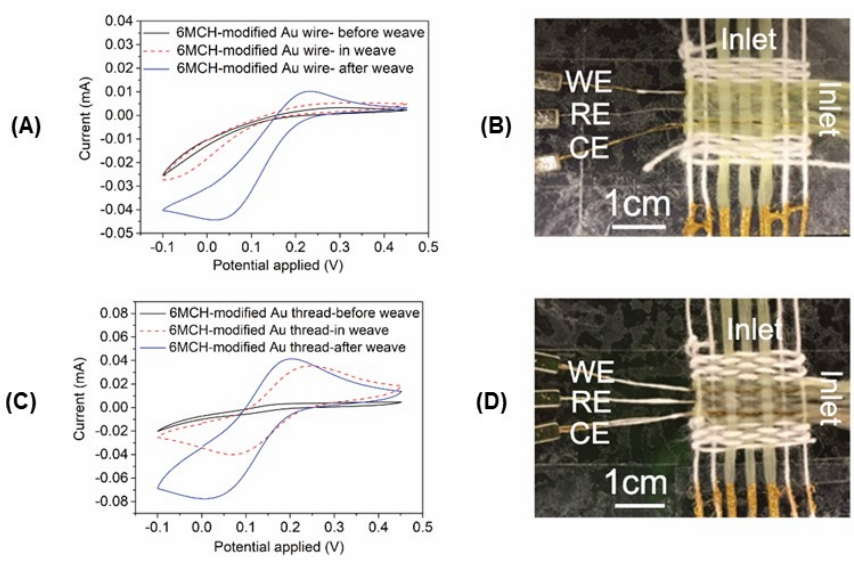

Figure 24. Electrochemical characterizations of microwire electrode-based woven devices (A) Representative cyclic voltammograms of the woven 6-MCH-modified gold microwire as a working electrode before weaving, in weave, and after removing from the weaves at 0.05 V/s scan rate. (B) Macroscopic photo of the microwire electrode-based woven device. (C) Representative cyclic voltammograms of the woven 6-MCH-modified gold thread as a working electrode before weaving, in weave, and after removing from weave electrodes. (D) Macroscopic photo of the thread electrode-based woven device. (Figure from **PAPER III**)

Integrated stem-loop probe E-DNA sensor into the microwire-based woven device, illustrated in Figure 25A, specifically detected unpurified, digested, and diluted (250-fold) RPA target amplicons. Figure 25B Indicates a statistically significant difference between the sample without DNA (only PBS(1X)), RPA blank, and target products. The signal suppression higher than 56% after 5 minutes of incubation of the sample was characterized as a positive test result. The whole system's detection limit was 10 copies/µL, as RPA amplified as few as this *S. epidermidis* genomic DNA concentration. The entire assay from RPA amplification to woven-based electrochemical detection required 65-70 minutes to be completed.

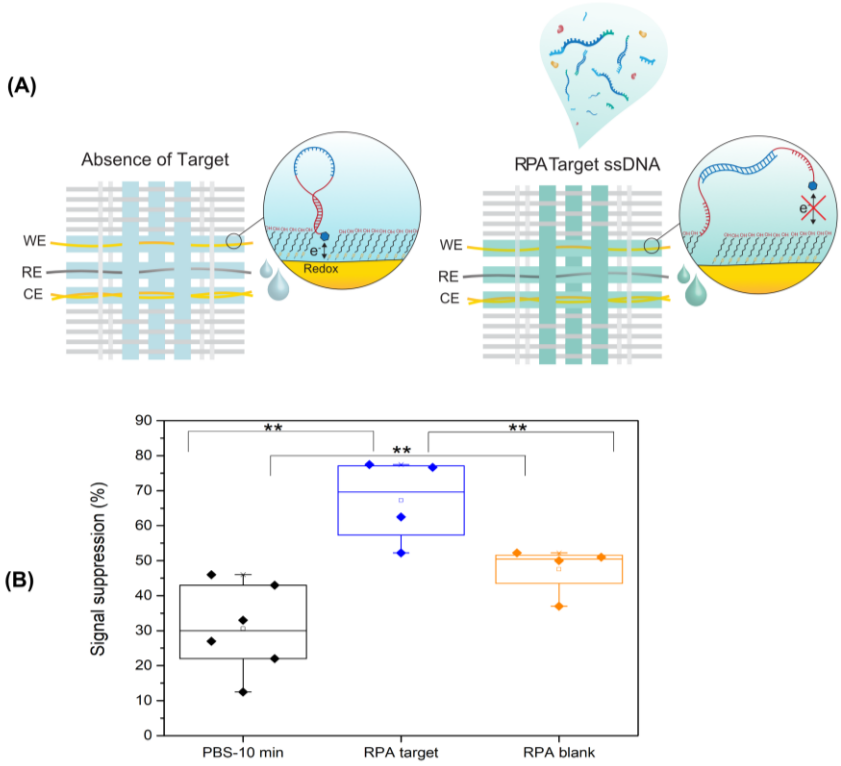

Figure 25. Integrated fiber-based electrochemical DNA (E-DNA) sensors (A) Illustration of the woven E-DNA sensor using stem-loop (S-L) DNA probe (B) Electrochemical responses of the woven E-DNA sensors to PBS (1X), RPA blank, and target products treated with exonuclease enzyme. ** significant at $p \leq 0.05$. (Figure from **PAPER III**)

Flexibility is a critical characteristic of fiber-based biosensors. Therefore, we evaluated the electrochemical performance of woven microwire and thread electrodes using the CV technique in straight, 90 degree-bend, and folded forms, as the woven devices were attached to a finger, see Figure 26B. The calculated current density (which is the ratio of the oxidation peak current of redox molecules in the corresponding CV scans to the electroactive surface area of the fiber-electrodes) of both unmodified fiber electrodes showed no statistically significant difference (p-values ≥ 0.05) for the examined devices at these three different forms, see Figure 26A. These results confirm the flexibility and robustness of the woven fiber electrodes for on-body electroanalytical applications, which paves the way for developing affordable and easy to manufacture analytical wearable diagnostics.

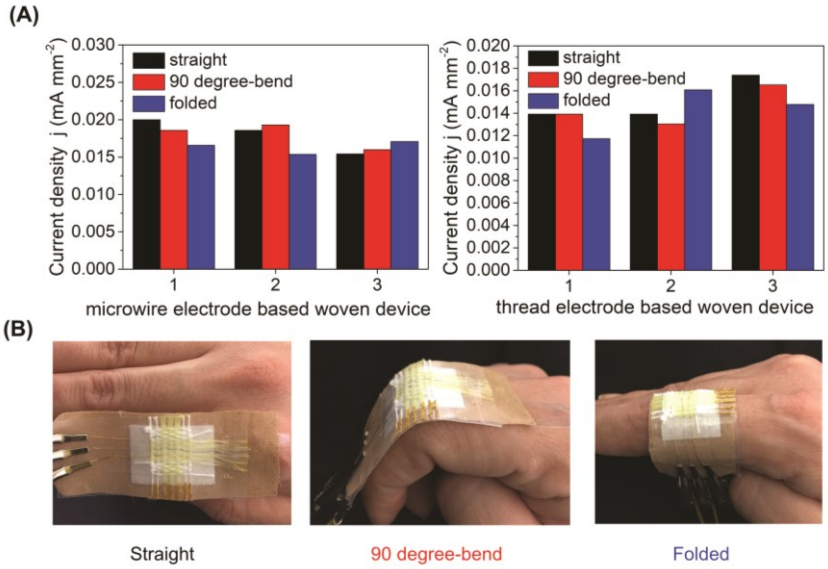

Figure 26. Flexibility characterization of the off-the-shelf woven thread (n = 3) and microwire electrodes (n = 3) on a finger of a human subject in three different forms: straight, 90 degree-bend and folded (A) Calculated current densities of the integrated fiber electrodes into the woven device (B) Photos of the actual woven fiber electrodes in the straight, 90 degree-bend and folded forms. (Figure from **PAPER III**)

This study showed the potential of using fiber-based material for scalable fabrication of electroanalytical devices for POC NAAT or other personalized diagnostic applications.

4.4.3 Paper-based electrochemical NAATs

In **PAPER IV**, we pursued further to fabricate a µPAD device that integrates electroanalytical DNA detection in a single paper-based device and combine that with RPA reaction on glass fiber substrates, in which RPA reagents were freeze-dried.

We chose the electrochemical sandwich hybridization assay to integrate into the µPAD device since (1) the SHA-based gold thread biosensors enable the detection of tailed dsDNA-RPA products, which eliminate the need for digesting step to obtain target ssDNAs; and (2) the sandwich-based detection offers two steps of hybridization due to the use of two different (capture and reporter) probes that make the assay highly specific.

We fabricated the SHA-based DNA sensors by immobilizing thiol-SAM capture probes on the off-the-shelf-gold threads, without the need for any types of beforehand cleaning of the electrodes. The CVs of the capture probe-modified gold threads verified the formation of the SAM on the electrode surface by showing the lower redox currents of potassium ferricyanide (5 mM), compared to the unmodified gold threads. This is due to the presence of the SAM on the electrode surface that impedes the efficient electron transfer between the redox molecules at electrode surfaces, see Figure 27A.

We characterized the performance of the electrochemical SHA-based DNA sensors in a tube-based system with RPA amplified target synthetic DNA (10 pM) of *O.* cf. *ovata* using a set of modified primers with single-stranded oligonucleotide tails. These tails at either strand of the dsDNA amplicons are complementary to the immobilized capture and HRP-modified reporter probe, see Figure 12. To do this, the purified dsDNA RPA amplicons were first pre-incubated in the HRP-modified reporter probes, prepared in skim milk (2%) and PBS solution, to allow hybridization of the tails of the RPA amplicons with the complementary HRP-labeled reporter probes. Then, the capture probe-modified gold threads were transferred to these pre-incubated samples. The presence of skim milk in this step prevents non-specific adsorption of the pre-incubated sample to the vacancies at the electrode surface by covering the unmodified sites at the electrode surface. Following the rinsing of the thread electrodes, we conducted the chronoamperometric measurements in a three-thread electrode setup (the RPA product-treated gold threads, a silver thread, and two gold threads were used as working, pseudo reference, and counter electrodes, respectively) after 5 minutes of incubation in TMB+H_2O_2 enzyme substrate. This enzymatic reaction between the HRP enzymes and TMB+H_2O_2 substrate led to more negative electrochemical currents after applying a reduction potential of -0.1 V to the working electrode. HRP catalyzes the oxidation of TMB molecules in the presence of H_2O_2 (Equation 7)[92], which can be recognized using electrochemical and colorimetric methods.[93,94] The obtained chronoamperometry currents after 1 second of the measurements showed a statistically significant difference between the RPA target and blank samples, see Figure 27B.

$$TMB_{(red)} + H_2O_2 \xrightarrow{HRP} TMB_{(ox)} + 2H_2O \qquad \text{(Equation 7)}$$

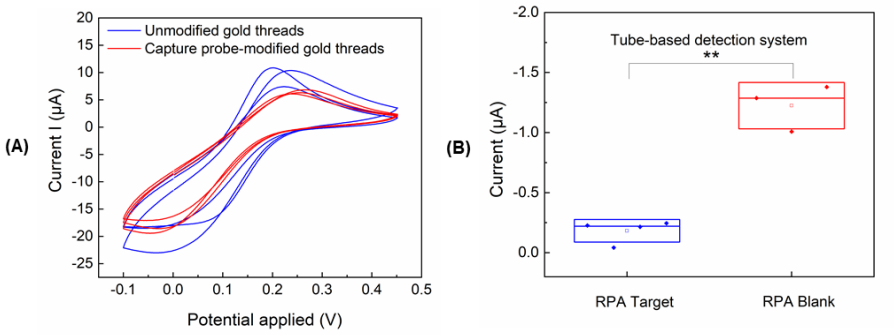

Figure 27. Representative cyclic voltammograms of (A) Capture probe-modified and unmodified gold threads (n=3) in the presence of 5 mM of potassium ferricyanide versus silver thread pseudo reference and gold thread counter electrodes at 0.05 V/s scan rate. (B) Chronoamperometric responses of SHA-based gold thread biosensors in the tube-based system using the thread electrode setup (n≥3). ** significant at $p \leq 0.05$.

Combining DNA isothermal amplification in the glass fiber substrates, for being detected by integrated electrochemical detection in µPADs requires several functions: (1) storing RPA reagents for the DNA amplification; (2) integrating SAM-based thread electrodes in the µPAD; (3) incubating samples in the device; (4) performing washing and transport of fluid steps within the device; and (5) performing electrochemical measurements in the µPAD.

In **PAPER IV**, we also tried to combine these steps most efficiently by fabricating a microfluidic paper-based DNA biosensor that was subsequently characterized with the unpurified RPA products obtained from RPA amplification in the glass fiber substrates. To integrate fluidic structures, we used wax printing and stacking techniques for creating channels and 3D-structuring the device. To integrate the electrochemical sensing, we incorporated the SHA-based DNA sensor into the paper device. To integrate valving, we used manual barriers in different layers of the device. In addition, the enormous design possibilities, which arise from tacking different paper layers in µPADs, enable the integration of specific functions in each layer of a single device. We exploited two types of papers: (1) cellulose filter, such as Whatman filter paper Grade 1; and (2) glass fiber filter as a non-cellulosic paper.

Our 3D-paper-based device had multilayer stacks of wax printed (and backed) Whatman filter paper to incorporate sample incubation, sample absorption, on-chip rinsing, and the three-electrode setup of thread electrodes for chronoamperometry measurements. Figure 28 illustrates the different layers of the device including: Layer 1 named as the sensor layer was a wax layer with a hallow channel, where the capture probe-modified gold thread (the working electrode) was placed; Layer 2 named as the capture layer was a filter paper with a hydrophilic paper channel used to incubate the RPA sample and subsequently wick the samples and Milli-Q water (at the further rinsing step) to an absorption layer underneath; Layer 3 named 1st blocking layer acted as a blocking fluidic valve, holding the samples at the incubation step for a certain period (30 minutes); Layer 4 was a glass fiber paper (pad) that served as an absorbent pad; Layer 5 was a second fluidic valve layer that prevented the fluid leakage from the absorbent pad (layer 4) to the following detection layers; Layer 6 and 7 functioned as detection layers that included two stacks of wax layers with hallow channel (as a spacer) and a hydrophilic filter paper (detection zone, where the thread counter and pseudo reference electrodes were located), respectively.

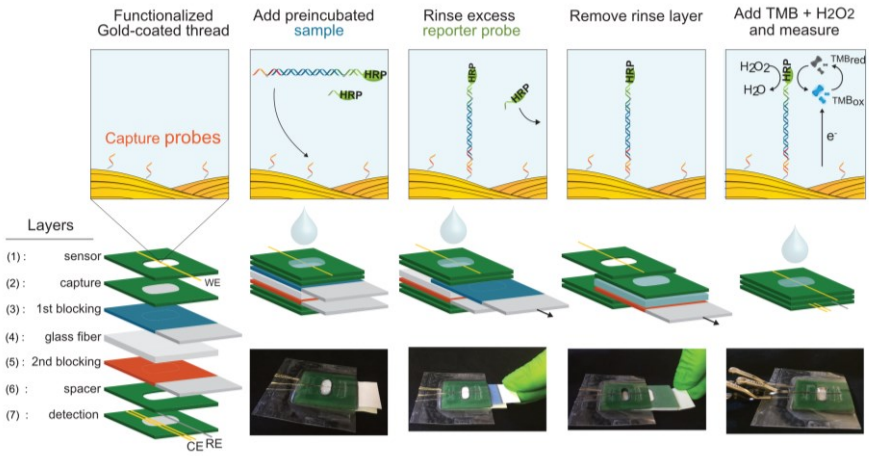

Figure 28. Illustration of different layers of the paper-based DNA sensors, their functions, and photos of the actual device at different steps of the sandwich hybridization assay.

As mentioned in *Section 2.4.3*, previous studies have shown that glass fiber paper is better suited for RPA reactions than cellulose filter paper. This finding was consistent with the obtained gel electrophoresis results of the freeze-dried based RPA amplification in Whatman filter paper Grade 1 and the glass fiber substrate, see Figure 29A. These results also showed that the freeze-dried RPA reagents in the glass fiber paper were still stable after one week of storing at -20 ℃, and the provided RPA products showed the target band at 145 bp. Therefore, we exploited the glass fiber papers for conducting the RPA reaction using the freeze-drying technique to store the amplification reagents in the substrates. After storage, we performed the RPA reaction for a series of concentrations of synthetic *O.* cf. *ovata* (10 pM-0. 001pM) and also purified genomic DNA of *O. cf. ovata* (1 ng/µL) and *O. cf. siamensis* (1 ng/µL) strains as target and negative control (non-target control) samples, by activating the stored RPA reagents and carrying out the reaction directly in the glass-fiber paper at a constant temperature of 37 ℃. Afterward, the glass fiber substrates were directly transferred to a solution containing the HRP modified-reporter probes, skim milk, and PBS buffer. At this pre-incubation step, the RPA products diffused into the solution and hybridized to the complementary HRP-probes. These steps involved no centrifugation or purification step. Figure 29A illustrates the gel electrophoresis of the RPA products (obtained from freeze-dried-based amplification in the glass fiber papers) after 30 minutes of pre-incubation with the HRP-modified capturing probe solution.

We characterized the performance of the integrated paper-based sensors with these pre-incubated RPA products by adding the samples to the inlet of the device and subsequently conducting the assay, including sample incubation, electrode washing, sample absorption, and chronoamperometric measurements on the device.

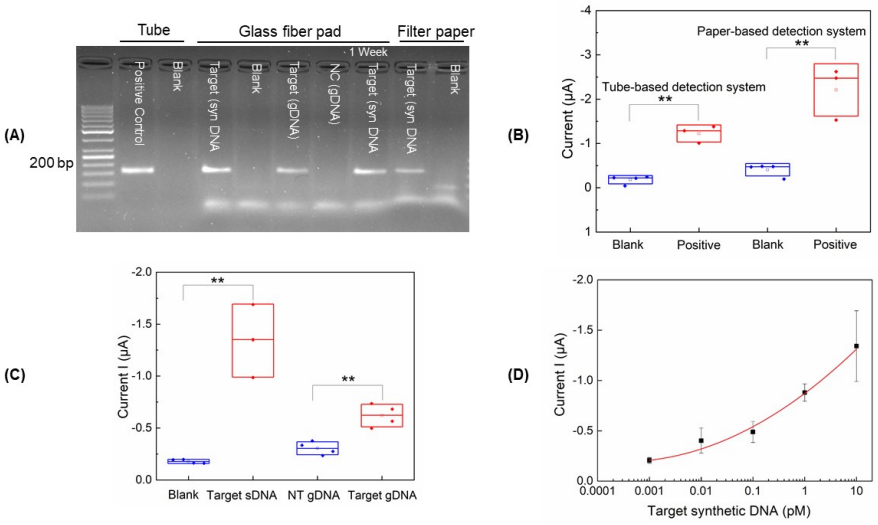

Figure 29. Characterization of the performance of the electrochemical SHA-based DNA sensors and the RPA reaction. (A) Gel electrophoresis of unpurified RPA products (target band at 145 bp) obtained from RPA reaction in tubes, glass fiber papers, and Whatman filter papers. (B) Chronoamperometric responses of the SHA-based gold thread DNA sensors (n≥3) in the tube-based and paper-based detection systems. (C) Chronoamperometric responses of the integrated paper-based SHA sensors (n≥3) to unpurified RPA products including blank, target synthetic DNA (Target sDNA: 10 pM), target genomic DNA (Target gDNA: 1 ng/μL), and negative control genomic DNA (NC gDNA:1 ng/μL) samples. (D) Calibration curve based on the responses of the integrated paper-based DNA sensors (n≥3) for the RPA products from 10 pM to 0.001 pM of target synthetic DNA. ** significant at p ≤0.05.

At the detection step, the increased currents caused by the enzymatic reaction of HRP and TMB+H_2O_2 substrate were measured by CA method. Figure 29D shows the calibration plot based on the responses of the integrated sensors to the different concentrations of amplified target synthetic DNAs in the glass fiber paper. The LOD of the integrated paper-based DNA sensor was 0.06 pM (see *Section 3.7.2*). The device could identify the RPA target products obtained with 10 pM of target synthetic and 1 ng/μL of target genomic DNA from the negative control genomic DNA (non-target DNA, 1 ng/μL) and the blank samples that contained nuclease-free water instead of DNA in the RPA reaction, see Figure 29C. Interestingly, the average response of the SHA-based gold thread sensors in the paper-based detection system was higher than the sensors examined in the tube-based system, see Figure 29B. This could be related to the different electrochemical behavior of the thread electrodes in the tube-based and paper-based systems or the use

of different volumes of the enzymatic substrate.[94] The paper-based electrochemical sensors identified 1 ng/μL target genomic DNA. The whole assay time from amplification to detection was 95 minutes.

In this study, we took advantage of different inherent features of porous paper substrates such as reagent storage, printability, and 3D manufacturing by stacking paper layers to fabricate an electroanalytical device for NAATs. This system eliminates the need for centrifugation and purification of the amplicons from the porous substrates. It minimizes manual interventions by enabling on-chip sample incubation, electrode rinsing, and electrochemical detection steps in a single paper-based device. For future work, we suggest incorporating glass fiber-based RPA amplification and off-chip pre-incubation steps into the integrated electrochemical DNA sensor.

5 Conclusions and Future work

This thesis presented the potential and applications of paper and textile materials to fabricate affordable, portable, and disposable microfluidic POC nucleic acid tests using inherent properties of fiber materials such as wicking, printability, and reagents storage. We integrated two types of electrochemical DNA sensors using a stem-loop probe and a sandwich hybridization assay into a woven textile microfluidic device and a 3D paper-based device, respectively. These fiber-based biosensors could specifically detect unpurified amplified genomic DNA of *S. epidermidis* (10 copies/µL) and *O. cf. ovata* (1 ng/µL) following recombinase polymerase amplification, a promising isothermal amplification method for POC NAATs. The LOD for these electrochemical fiber-based biosensors was much lower than previously reported paper-based and thread-based POC NAAT sensors, which are amplification-free, thus too high for clinical sample detection. In addition, the assays require 75-95 minutes to be completed. Although this turnaround time is close to that of conventional NAATs (e.g., qPCR), the presented assays require less instrumentation and are more sustainable.

Considering the vast potential of fiber materials for applications in POC diagnostics, future work can focus on two following approaches:

First, fabricating fully automated, sample-to-answer, paper/thread-based microfluidic electroanalytical devices for POC NAATs. This can include 1) rolling thread-based devices for continuous detection of pathogens and 2) integrated paper-based devices that perfume sample preparation, amplification, and detection steps in a single device. These automated devices can be readily connected to handheld electronic tools[95] (e.g., smartphones) to carry out measurements, analyze, and store or transfer data.

Second, the presented textile materials, including off-the-shelf conducting thread electrodes and fast-wicking threads, provide promising platforms for readily and at scale fabrication of 3D microfluidic devices with diverse and complex patterns, not only for wearable diagnostic applications but for developing miniaturized analytical devices for self-testing or environmental monitoring. Additionally, creating textile-based organic electrochemical transistors (OECTs) is an interesting example of using presented textile materials that offer highly sensitive and specific multiplex analytical systems for POC diagnostic applications.

6 Acknowledgment

I would like to sincerely thank my supervisor, Assoc. Prof. Mahiar Max Hamedi for giving me the opportunity to conduct my Ph.D. studies at Hamedi Lab and being his first Ph.D. student. Thank you, Mahiar, for all your support, guidance, encouragement, and creative ideas throughout my research at KTH. I would like to send my great gratitude to Assoc. Prof. Anna Herland for all her invaluable help, insights and mentorship over the course of my Ph.D. journey. I also would like to acknowledge professor Lars Wågberg for all his advice and guidance throughout my research at Fiber and Polymer Technology Department.

Furthermore, I wish to thank all the present and former colleagues and friends at the FPT department, Herland Lab, and in particular, Hamedi Lab specifically in the iMDx group: Martin, Georgios, Anna.T, Pedro, Liangqi, Andrew and Ingrid, for creating a friendly, constructive, and supportive atmosphere. Thank you all for all our wonderful memories. Also, I would like to thank my former advisor, Dr. Somayeh Akbari, in my Master's studies at AUT, my first-grade teacher Mrs. Mehrtaj and all my teachers and mentors, who played key roles in my academic life.

The European Research Council and the Knut and Alice Wallenberg Foundation are acknowledged for their financial support.

Finally, I would like to express my greatest appreciation to my dearest parents, beloved brother, Amir Saleh and my sweetheart aunt, Nouri Naaz, for their lifetime endless support and love. Likewise, I would like to thank my husband´s parents, sister-in-law Roja, and brother-in-law Sajjad for their encouragement and cordiality.

Last but not least, I would like to thank my dearly beloved husband, Mohammad, from the bottom of my heart for his patience, unconditional love, understanding, and being my biggest support throughout my Ph.D. studies and in our married life.

7 References

1 Patabadige, D. E. et al. Micro total analysis systems: fundamental advances and applications. Analytical chemistry 88, 320-338 (2016).

2 Mitra, S. K. & Chakraborty, S. Microfluidics and nanofluidics handbook: fabrication, implementation, and applications. (CRC press, 2016).

3 Zhang, J., Chen, K. & Fan, Z. Circulating tumor cell isolation and analysis. Advances in clinical chemistry 75, 1-31 (2016).

4 Becker, H., Hansen-Hagge, T. & Gärtner, C. Microfluidic devices for rapid identification and characterization of pathogens. Biological Identification, 220-249 (2014).

5 Samandari, M., Julia, M. G., Rice, A., Chronopoulos, A. & Armando, E. Liquid biopsies for management of pancreatic cancer. Translational Research 201, 98-127 (2018).

6 Issadore, D. & Westervelt, R. M. Point-of-care Diagnostics on a Chip. (Springer Science & Business Media, 2013).

7 Kozel, T. R. & Burnham-Marusich, A. R. Point-of-care testing for infectious diseases: past, present, and future. Journal of clinical microbiology 55, 2313 (2017).

8 Chin, C. D., Chin, S. Y., Laksanasopin, T. & Sia, S. K. in Point-of-care diagnostics on a chip 3-21 (Springer, 2013).

9 Liu, J., Geng, Z., Fan, Z., Liu, J. & Chen, H. Point-of-care testing based on smartphone: The current state-of-the-art (2017–2018). Biosensors and Bioelectronics 132, 17-37 (2019).

10 Christodouleas, D. C., Kaur, B. & Chorti, P. From point-of-care testing to eHealth diagnostic devices (eDiagnostics). ACS central science 4, 1600-1616 (2018).

11 Mauk, M. G., Song, J., Liu, C. & Bau, H. H. Simple approaches to minimally-instrumented, microfluidic-based point-of-care nucleic acid amplification tests. Biosensors 8, 17 (2018).

12 Rong, Z. et al. Smartphone-based fluorescent lateral flow immunoassay platform for highly sensitive point-of-care detection of Zika virus nonstructural protein 1. Analytica chimica acta 1055, 140-147 (2019).

13 Holland, C. A. & Kiechle, F. L. Point-of-care molecular diagnostic systems—past, present and future. Current opinion in microbiology 8, 504-509 (2005).

14 Van Nguyen, H. et al. Nucleic acid diagnostics on the total integrated lab-on-a-disc for point-of-care testing. Biosensors and Bioelectronics 141, 111466 (2019).

15 Rodriguez-Manzano, J. et al. Handheld point-of-care system for rapid detection of SARS-CoV-2 extracted RNA in under 20 min. ACS central science 7, 307-317 (2021).
16 Besurence, A. T. A. Know your body, plan your future: Rapid diagnostic tests-made in Austria, <https://www.besurence.com/en/corona-test/covid-19-antigen/> (2021).
17 Lisowski, P. & Zarzycki, P. K. Microfluidic paper-based analytical devices (μPADs) and micro total analysis systems (μTAS): development, applications and future trends. Chromatographia 76, 1201-1214 (2013).
18 Wang, S., Chinnasamy, T., Lifson, M. A., Inci, F. & Demirci, U. Flexible substrate-based devices for point-of-care diagnostics. Trends in biotechnology 34, 909-921 (2016).
19 Hu, J. et al. Advances in paper-based point-of-care diagnostics. Biosensors and Bioelectronics 54, 585-597 (2014).
20 Farajikhah, S., Cabot, J. M., Innis, P. C., Paull, B. & Wallace, G. Life-saving threads: advances in textile-based analytical devices. ACS combinatorial science 21, 229-240 (2019).
21 Gong, M. M. & Sinton, D. Turning the page: advancing paper-based microfluidics for broad diagnostic application. Chemical reviews 117, 8447-8480 (2017).
22 Choi, J. R. et al. based sample-to-answer molecular diagnostic platform for point-of-care diagnostics. Biosensors and Bioelectronics 74, 427-439 (2015).
23 Hamedi, M. M. et al. Integrating electronics and microfluidics on paper. Advanced Materials 28, 5054-5063 (2016).
24 Merck Research. Development. Production. Filter Paper, <https://www.sigmaaldrich.com/SE/en/products/filtration/filter-paper> (2021, July).
25 Ainla, A., Hamedi, M. M., Güder, F. & Whitesides, G. M. Electrical textile valves for paper microfluidics. Advanced Materials 29, 1702894 (2017).
26 Mondal, S., Zehra, N., Choudhury, A. & Iyer, P. K. Wearable Sensing Devices for Point of Care Diagnostics. ACS Applied Bio Materials (2020).
27 Economou, A., Kokkinos, C. & Prodromidis, M. Flexible plastic, paper and textile lab-on-a chip platforms for electrochemical biosensing. Lab on a Chip 18, 1812-1830 (2018).
28 Öberg Månsson, I., Piper, A. & Hamedi, M. M. Weaving Off-The-Shelf Yarns into Textile Micro Total Analysis Systems (μTAS). Macromolecular Bioscience 20, 2000150 (2020).

29 Tang, R. H. et al. Advances in paper-based sample pretreatment for point-of-care testing. Critical reviews in biotechnology 37, 411-428 (2017).
30 Bender, A. T. Sample Preparation for Point-of-Care Nucleic Acid Amplification Testing of Bloodborne Viruses, (2020).
31 Peluso, A. L. et al. Use of FTA cards for the storage of breast carcinoma nucleic acid on fine‐needle aspiration samples. Cancer cytopathology 123, 582-592 (2015).
32 Ndunguru, J. et al. Application of FTA technology for sampling, recovery and molecular characterization of viral pathogens and virus-derived transgenes from plant tissues. Virology Journal 2, 1-12 (2005).
33 Byrnes, S. et al. One-step purification and concentration of DNA in porous membranes for point-of-care applications. Lab on a Chip 15, 2647-2659 (2015).
34 Govindarajan, A., Ramachandran, S., Vigil, G., Yager, P. & Böhringer, K. in 2011 IEEE 24th International Conference on Micro Electro Mechanical Systems. 932-935 (IEEE).
35 Kolluri, N. et al. SNAPflex: a paper-and-plastic device for instrument-free RNA and DNA extraction from whole blood. Lab on a Chip 20, 3386-3398 (2020).
36 McFall, S. M. et al. A simple and rapid DNA extraction method from whole blood for highly sensitive detection and quantitation of HIV-1 proviral DNA by real-time PCR. Journal of virological methods 214, 37-42 (2015).
37 Sullivan, B. P., Bender, A. T., Ngyuen, D. N., Zhang, J. Y. & Posner, J. D. Nucleic acid sample preparation from whole blood in a paper microfluidic device using isotachophoresis. Journal of Chromatography B 1163, 122494 (2021).
38 Carrell, C. et al. Beyond the lateral flow assay: A review of paper-based microfluidics. Microelectronic Engineering 206, 45-54 (2019).
39 Kaur, N. & Toley, B. J. based nucleic acid amplification tests for point-of-care diagnostics. Analyst 143, 2213-2234 (2018).
40 Krsek, M. & Wellington, E. Comparison of different methods for the isolation and purification of total community DNA from soil. Journal of Microbiological methods 39, 1-16 (1999).
41 Naik, P., Manna, R. & Paul, D. in Paper Microfluidics 115-146 (Springer, 2019).
42 Craw, P. & Balachandran, W. Isothermal nucleic acid amplification technologies for point-of-care diagnostics: a critical review. Lab on a Chip 12, 2469-2486 (2012).

43 Lee, S. H. et al. Emerging ultrafast nucleic acid amplification technologies for next-generation molecular diagnostics. Biosensors and Bioelectronics 141, 111448 (2019).
44 Giuffrida, M. C. & Spoto, G. Integration of isothermal amplification methods in microfluidic devices: Recent advances. Biosensors and Bioelectronics 90, 174-186 (2017).
45 Magro, L. et al. Paper microfluidics for nucleic acid amplification testing (NAAT) of infectious diseases. Lab on a Chip 17, 2347-2371 (2017).
46 Zanoli, L. M. & Spoto, G. Isothermal amplification methods for the detection of nucleic acids in microfluidic devices. Biosensors 3, 18-43 (2013).
47 Seok, Y. et al. A paper-based device for performing loop-mediated isothermal amplification with real-time simultaneous detection of multiple DNA targets. Theranostics 7, 2220 (2017).
48 Linnes, J., Rodriguez, N., Liu, L. & Klapperich, C. Polyethersulfone improves isothermal nucleic acid amplification compared to current paper-based diagnostics. Biomedical microdevices 18, 30 (2016).
49 Rodriguez, N. M. et al. based RNA extraction, in situ isothermal amplification, and lateral flow detection for low-cost, rapid diagnosis of influenza A (H1N1) from clinical specimens. Analytical chemistry 87, 7872-7879 (2015).
50 Lobato, I. M. & O'Sullivan, C. K. Recombinase polymerase amplification: basics, applications and recent advances. Trac Trends in analytical chemistry 98, 19-35 (2018).
51 GE Healthcare Life Sciences. (2021).
52 Rohrman, B. A. & Richards-Kortum, R. R. A paper and plastic device for performing recombinase polymerase amplification of HIV DNA. Lab on a chip 12, 3082-3088 (2012).
53 Cordray, M. S. & Richards-Kortum, R. R. A paper and plastic device for the combined isothermal amplification and lateral flow detection of Plasmodium DNA. Malaria journal 14, 1-8 (2015).
54 Karlikow, M. & Pardee, K. in Paper-based Diagnostics 171-201 (Springer, 2019).
55 Connelly, J. T., Rolland, J. P. & Whitesides, G. M. "Paper machine" for molecular diagnostics. Analytical chemistry 87, 7595-7601 (2015).
56 Scida, K., Li, B., Ellington, A. D. & Crooks, R. M. DNA detection using origami paper analytical devices. Analytical chemistry 85, 9713-9720 (2013).
57 Yamada, K., Shibata, H., Suzuki, K. & Citterio, D. Toward practical application of paper-based microfluidics for medical diagnostics: state-of-the-art and challenges. Lab on a Chip 17, 1206-1249 (2017).

58 Jauset-Rubio, M. et al. Ultrasensitive, rapid and inexpensive detection of DNA using paper based lateral flow assay. Scientific reports 6, 1-10 (2016).
59 Song, Y. et al. Visual detection of DNA on paper chips. Analytical chemistry 86, 1575-1582 (2014).
60 Xu, G. et al. Paper‐Origami‐Based Multiplexed Malaria Diagnostics from Whole Blood. Angewandte Chemie 128, 15476-15479 (2016).
61 Rafique, B., Iqbal, M., Mehmood, T. & Shaheen, M. A. Electrochemical DNA biosensors: A review. Sensor Review (2019).
62 Wu, Q., Zhang, Y., Yang, Q., Yuan, N. & Zhang, W. Review of electrochemical DNA biosensors for detecting food borne pathogens. Sensors 19, 4916 (2019).
63 Liu, A. et al. Development of electrochemical DNA biosensors. TrAC Trends in Analytical Chemistry 37, 101-111 (2012).
64 Kavita, V. DNA biosensors-a review. J. Bioeng. Biomed. Sci 7, 222 (2017).
65 Blair, E. O. & Corrigan, D. K. A review of microfabricated electrochemical biosensors for DNA detection. Biosensors and Bioelectronics 134, 57-67 (2019).
66 Rashid, J. I. A. & Yusof, N. A. The strategies of DNA immobilization and hybridization detection mechanism in the construction of electrochemical DNA sensor: A review. Sensing and bio-sensing research 16, 19-31 (2017).
67 Hvastkovs, E. G. & Buttry, D. A. Recent advances in electrochemical DNA hybridization sensors. Analyst 135, 1817-1829 (2010).
68 Cunningham, J. C., Brenes, N. J. & Crooks, R. M. Paper electrochemical device for detection of DNA and thrombin by target-induced conformational switching. Analytical chemistry 86, 6166-6170 (2014).
69 Karim, N. et al. Scalable production of graphene-based wearable e-textiles. ACS nano 11, 12266-12275 (2017).
70 Kim, J., Kumar, R., Bandodkar, A. J. & Wang, J. Advanced materials for printed wearable electrochemical devices: A review. Advanced Electronic Materials 3, 1600260 (2017).
71 Pensa, E. et al. The chemistry of the sulfur–gold interface: in search of a unified model. Accounts of chemical research 45, 1183-1192 (2012).
72 Xue, Y., Li, X., Li, H. & Zhang, W. Quantifying thiol–gold interactions towards the efficient strength control. Nature communications 5, 1-9 (2014).
73 Love, J. C., Estroff, L. A., Kriebel, J. K., Nuzzo, R. G. & Whitesides, G. M. Self-assembled monolayers of thiolates on metals as a form of nanotechnology. Chemical reviews 105, 1103-1170 (2005).

74 Fosdick, S. E. et al. Wire, mesh, and fiber electrodes for paper-based electroanalytical devices. Analytical chemistry 86, 3659-3666 (2014).
75 Adkins, J. A. & Henry, C. S. Electrochemical detection in paper-based analytical devices using microwire electrodes. Analytica chimica acta 891, 247-254 (2015).
76 Mao, X., Du, T.-E., Wang, Y. & Meng, L. Disposable dry-reagent cotton thread-based point-of-care diagnosis devices for protein and nucleic acid test. Biosensors and Bioelectronics 65, 390-396 (2015).
77 Otto, M. Staphylococcus epidermidis—the'accidental'pathogen. Nature reviews microbiology 7, 555-567 (2009).
78 Oliveira, W. et al. Staphylococcus aureus and Staphylococcus epidermidis infections on implants. Journal of Hospital Infection 98, 111-117 (2018).
79 Berdalet, E. et al. Harmful algal blooms in benthic systems: Recent progress and future research. Oceanography 30, 36-45 (2017).
80 Josephs, E. A., Ye, T., Josephs, E. & Ye, T. Nanoscale Spatial Distribution of Tethered DNA on Model Nucleic Acid Sensor Surfaces.
81 West, R. M. Electrical Manipulation of DNA Self-Assembled Monolayers: Electrochemical Melting of Surface-Bound DNA. Journal of The Electrochemical Society 167, 037544 (2020).
82 Xiao, Y., Lai, R. Y. & Plaxco, K. W. Preparation of electrode-immobilized, redox-modified oligonucleotides for electrochemical DNA and aptamer-based sensing. Nature protocols 2, 2875 (2007).
83 Martin, S. H. Papain-digestion. The Journal of physiology 5, 213 (1885).
84 Van der Hoorn, R. A. Plant proteases: from phenotypes to molecular mechanisms. Annu. Rev. Plant Biol. 59, 191-223 (2008).
85 Ezaki, T. & Suzuki, S. Achromopeptidase for lysis of anaerobic gram-positive cocci. Journal of clinical microbiology 16, 844-846 (1982).
86 Buser, J. R. et al. A disposable chemical heater and dry enzyme preparation for lysis and extraction of DNA and RNA from microorganisms. Analytical Methods 8, 2880-2886 (2016).
87 Heiniger, E. K. et al. Comparison of point-of-care-compatible lysis methods for bacteria and viruses. Journal of microbiological methods 128, 80-87 (2016).
88 Towbin, H., Staehelin, T. & Gordon, J. Electrophoretic transfer of proteins from polyacrylamide gels to nitrocellulose sheets: procedure and some applications. Proceedings of the national academy of sciences 76, 4350-4354 (1979).
89 Cheng, C. M. et al. Paper ‐ based ELISA. Angewandte Chemie 122, 4881-4884 (2010).

90 Ferguson, B. S. et al. Integrated microfluidic electrochemical DNA sensor. Analytical chemistry 81, 6503-6508 (2009).
91 Fu, E., Ramsey, S. A., Kauffman, P., Lutz, B. & Yager, P. Transport in two-dimensional paper networks. Microfluidics and nanofluidics 10, 29-35 (2011).
92 Bettazzi, F., Romero Natale, A., Torres, E. & Palchetti, I. Glyphosate determination by coupling an immuno-magnetic assay with electrochemical sensors. Sensors 18, 2965 (2018).
93 Fanjul-Bolado, P., González-García, M. B. & Costa-García, A. Amperometric detection in TMB/HRP-based assays. Analytical and Bioanalytical chemistry 382, 297-302 (2005).
94 Baldrich, E., del Campo, F. J. & Muñoz, F. X. Biosensing at disk microelectrode arrays. Inter-electrode functionalisation allows formatting into miniaturised sensing platforms of enhanced sensitivity. Biosensors and Bioelectronics 25, 920-926 (2009).
95 Ainla, A. et al. Open-source potentiostat for wireless electrochemical detection with smartphones. Analytical chemistry 90, 6240-6246 (2018).